Acta Geochim
https://doi.org/10.1007/s11631-020-00403-9

ORIGINAL ARTICLE

Mineralogy and geochemistry of pozzolans from the Tombel Plain, Bamileke Plateau, and Noun Plain monogenetic volcanoes in the central part of the Cameroon Volcanic Line

Mbowou Ngantche Igor Fulbert[1,2] · Owona Sébastien[1] · Chako Tchamabe Boris[3] · Lissom Justin[1] · Lanson Bruno[4] · Ekodeck Georges Emmanuel[5]

Received: 20 September 2019 / Revised: 2 January 2020 / Accepted: 28 January 2020

Abstract Pozzolans from the Tombel Plain, Bamileke Plateau, and Noun Plain, 3 monogenetic volcanic fields in the central part of the Cameroon Volcanic Line (the Tombel Plain, Bamileke Plateau, and Noun Plain), were explored in order to constrain their petrology and make some predictions on their pozzolanicity. The rocks in this study include alkaline and subalkaline basalts, trachybasalts, and basanites. Most of these rocks present an overall composition that overlaps with primitive mantle, suggesting rapid ascent of magmas, limited crustal contamination and crystal fractionation of olivine, clinopyroxene, and feldspar. The pozzolans present enrichment of LREE relative to HREE and high chondrite normalized ratios of La/Yb and Tb/Yb, ranging between 7 and 20 and > 1.9 respectively, similar to those of Ocean Island Basalts. Like other nearby volcanoes, partial melting in a dominantly garnet-bearing mantle zone can be assumed. Quantitative mineralogy by X-ray diffraction revealed various mineral phases with dominantly plagioclase, augite, olivine, and Fe–Ti oxides. The samples contains important amorphous phase up to 23, 51, and 69 wt% in the Tombel Plain, Noun Plain, and Bamileke Plateau, respectively. This elevated amount of amorphous phases together with the sum of SiO_2, Al_2O_3, and total Fe_2O_3 (SAI = 68.50–83.50 > 70 wt%) according to ASTM C 618 standard and the sum of CaO, FeO, and MgO (CIM = 14.5–30.52 wt% and 23.58–31.08 wt%) suggest interesting pozzolanicity character for the studied pozzolans.

Keywords Pozzolans · Mineralogy · Geochemistry · Pozzolanicity · Monogenetic volcanic fields · Cameroon Volcanic Line

1 Introduction

Pozzolans are unconsolidated pyroclastic rocks or tephra, resulting from "dry" explosive magmatism and consist mostly of juvenile components such as scoria, free crystal, and volcanic glass that vary in size, color, shape, and texture (Morrissey et al. 2000). Pozzolans have been identified in various locations along the Cameroon Volcanic Line (CVL) notably at volcanic cones in monogenetic fields in the Tombel Plain (Nkouathio 2006; Nkouathio et al. 2008; Tchamdjou et al. 2017), Baleng lake within Bamileke plateau and in Noun Plain (Wotchoko et al. 2005).

Monogenetic volcanoes of the CVL display incomplete magmatic suites limited to basanites, basalts, and accessory hawaiites while polygenetic volcanoes are characterized by a complete magmatic series (Sato et al. 1990; Déruelle

Electronic supplementary material The online version of this article (https://doi.org/10.1007/s11631-020-00403-9) contains supplementary material, which is available to authorized users.

✉ Owona Sébastien
owonas2012@gmail.com; owonas@univ-douala.com; owonas@yahoo.fr

[1] Faculty of Science, Department of Earth Sciences, University of Douala, P.O. Box 24157, Douala, Cameroon

[2] Faculty of Science, Department of Geology, University of Buea, P.O. Box 63, Buea, Cameroon

[3] CONACYT-Centro de Ingenieria y Desarrollo Industrial (Sede Campeche), Av. Playa Pie de la Cuesta N° 702, Desarrollo San Pablo, P.O. Box. 76125, Querétaro, Mexico

[4] Institut des Sciences de la Terre (ISTerre), Maison des Sciences de la Terre, P.O. Box 53, 38041 Grenoble Cedex 9, France

[5] Faculty of Science, Department of Earth Sciences, University of Yaoundé I, P.O. Box: 812, Yaoundé, Cameroon

Published online: 12 February 2020

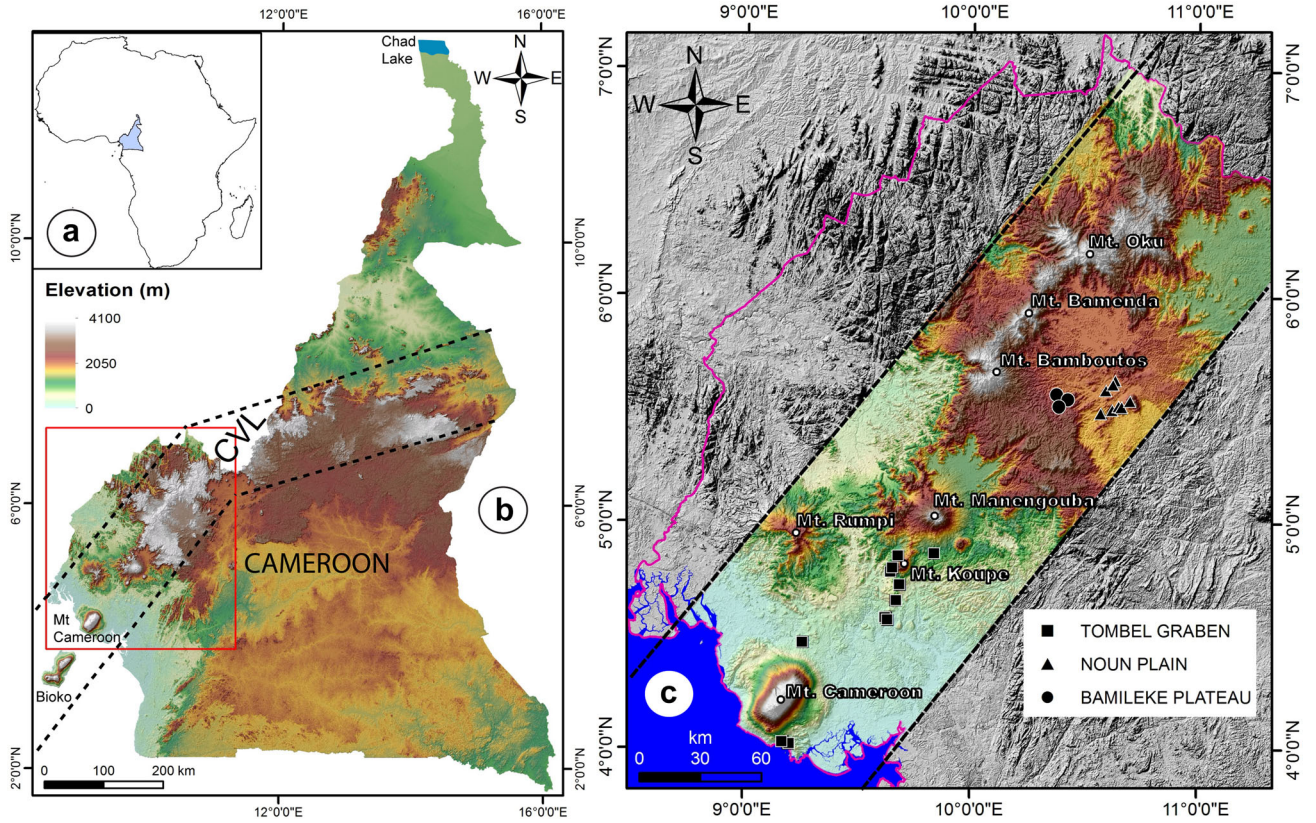

Fig. 1 **a** Location of Cameroon in Africa. **b** The Cameroon Volcanic Line (CVL) and **c** sampling map of pyroclastic rocks (pozzolans) along the central part of CVL

et al. 2007; Chako Tchamabe 2014; Tiabou et al. 2019). Monogenetic volcanoes in the world are known to be geochemically and volcanologically simpler (Brenna et al. 2010) and smaller in terms of volume of magma erupted as compared to polygenetic volcanoes. Heterogeneity of the mantle under some volcanoes has been pointed out as the source of slight differences, notably on MgO content, observed on the composition of the lavas belonging to monogenetic volcanic cones or field. This has been reported for example at the Crater Hill volcano in New Zealand (Smith et al. 2008), the Udo tuff in South Korea (Brenna et al. 2010), the Parìcutin in the Michoacán-Guanajuato volcanic field in Mexico (Erlund et al. 2010), the Auckland volcanic field in New Zealand (McGee et al. 2012, 2013), the Mt Gambier Complex in Australia (Van Otterloo et al. 2014), the Barombi Mbo Maar complex (Chako Tchamabe 2014), the Debunscha Maar complex (Ngwa et al. 2017), and the Baossi—Warack volcanoes (Tiabou et al. 2019) in Cameroon (Central Africa). Some of these compositional differences result from successive partial melting of distinct but contiguous source with varying composition (McGee et al. 2012, 2013; McGee and Smith 2016), from polycyclic activity of the volcanoes that will enable deposition, through the same vent, of lavas originated from distinct magmas derived from mantle zones with slightly different percentage of garnet (Chako Tchamabe 2014) or, most of time, lavas resulting from mixing of two or many batches of magma of different composition (Erlund et al. 2010, Otterloo et al. 2014; Ngwa et al. 2017; Tiabou et al. 2019).

Numerous studies done on monogenetic volcanoes have shown that products from their eruption are lava flows and pyroclastic materials from a strombolian eruptive style as well as phreatomagmatic deposits (Nemeth et al. 2003; Martin and Nemeth 2006; Valentine et al. 2007; Kereszturi et al. 2011; Nemeth and Kereszturi 2015).

Most of the petrogenetic studies done, on monogenetic volcanoes along the CVL have focussed mostly on lava flow and cinder cones (Tiabou et al. 2015, 2019; Sato et al. 1990) and maar diatreme volcanoes such as Nyos (Aka et al. 2004, 2008; Hasegawa et al. 2019), Barombi Kotto lake (Tamen et al. 2007; Asaah et al. 2020), Lakes Elum, Wum and Oku (Asaah et al. 2015), and Debunscha (Ngwa et al. 2017). Little attention has been paid to the geochemistry of these pyroclastic materials, at least in some volcanic Plateau (Wandji et al. 2000, Wotchoko et al. 2005). However, nothing has been done on the pozzolanic monogenetic cones identified so far along the line.

Fig. 2 Photographs showing some outcrops of the studied pozzolans. **a** Reddish to medium brown stratified deposits in the Tombel Plain; **b** Reddish to medium brown and Black pozzolan deposit surrounding Baleng Crater Lake in the Bamileke Plateau, **c** deposits showing an alternating beds of fine-grained "reddish" (dark brown) and coarse-grained black pozzolan at Foumbot quarry (Noun Plain); **d** Uniform black pozzolan in front of Petpounoun lake (Noun Plain); **e** Dark yellow—colored pozzolans materials that constitute a soil of Monoun village (Noun Plain) and follows topography

Furthermore, no study has been carried out to point out possible petrological links amongst these pozzolanic cones with nearby volcanoes.

Most of these cones, especially those in the Tombel graben, like the Djoungo volcanic cone, are currently exploited, and their pozzolans used as an additive to clinker in the manufacturing of pozzolanic cement in local cement factories (Billong et al. 2013; Tchamdjou et al. 2017). The pozzolanicity or pozzolanic activity of natural pozzolan refers to both its capacity of binding lime and the rate at which the binding reaction takes place (Pichon 1994; Segui 2011; Walker and Pavía 2011). This characteristic depends

Table 1 Physical and LOI characteristics of the Tombel Plain, Bamileke Plateau, and Noun Plain pozzolans

Unit	Location	Sample number	Latitudes	Longitudes	Elevation (m)	Petrography	Apparent colour	Colour	Nitrogen 105 (wt%)	Oxygen 1000 (wt%)	Oxygen 500 (wt%)	Total LOI
Tombel plain	Barombi Kotto Island	Bki48	N 4°28′6.1″	E 9°15′45″	102	BA	Darkish	Dark green grey	5.31	0.34	3	8.64
		Bki49	N 4°28′10.5″	E 9°15′46.4″	116	AB	Darkish	Medium grey	0.38	− 0.28	0.38	0.48
		Bki50	N 4°28′4.6″	E 9°15′50.3″	105	AB	Reddish	Dark green grey	0.38	− 0.38	0.36	0.37
	Limbe town	Lim51	N 4°1′6.5″	E 9°12′4.8″	36	AB	Yellowish	Dark red brown	0.25	0.05	0.56	0.87
		Lim52	N 4°1′6.5″	E 9°12′4.8″	36	AB	Reddish	Medium brown	0.27	0.06	0.37	0.7
		Lim53	N 4°1′41.5″	E 9°10′42.8″	165	AB	Darkish	Black	0.31	− 0.45	0.11	− 0.03
		Lim54	N 4°1′41.5″	E 9°10′42.8″	167	AB	Reddish	Dark orange brown	0.57	− 0.41	0.95	1.12
	Mont Koupe	Kpé02	N 4°47′3.7″	E 9°39′3.6″	518	AB	Darkish	Medium grey	1.08	− 0.4	0.66	1.34
		Kpé04	N 4°51′3.7″	E 9°40′54.3″	813	AB	Reddish	Medium brown	0.26	0	0.3	0.56
		Kpé05	N 4°51′3.7″	E 9°40′54.3″	813	AB	Yellowish	Light yellow brown	2.24	− 0.06	1.58	3.76
		Kpé06	N 4°51′3.7″	E 9°40′54.3″	813	AB	Darkish	Dark olive	2.20	− 0.38	1.04	2.86
		Kpé07	N 4°47′41.8″	E 9°39′27.8″	654	SAB	Darkish	Dark grey	− 0.08	− 0.71	0.42	− 0.37
	Tombel town	TL08	N 4°43′25.8″	E 9°41′25.0″	455	SAB	Darkish	Dark green grey	2.27	− 0.41	1.59	3.45
		TL09	N 4°43′25.8″	E 9°41′25.0″	455	SAB	Darkish	Light yellow grey	3.67	− 0.27	2.29	5.68
		TL10	N 4°43′25.8″	E 9°41′25.0″	455	AB	Darkish	Dark green grey	1.34	− 0.5	0.63	1.47
	Penja-Djombe	TPja13	N 4°39′18.8″	E 9°40′12.0″	259	AB	Red-Darkish	Dark green brown	4.58	− 0.07	2.7	7.21
		TDJ14	N 4°34′6.3″	E 9°38′15.4″	97	TB-H	Darkish	Light green grey	0.07	− 0.33	0.04	− 0.22
		TDJ15	N 4°34′6.3″	E 9°38′15.4″	97	TB-H	Reddish	Light brown	0.15	− 0.12	0.21	0.25
		TDJ16	N 4°34′6.3″	E 9°38′15.4″	97	TB-H	Darkish	Dark green grey	1.23	− 0.32	1.02	1.92
	Mombo	TMC17	N 4°34′48.4″	E 9°37′43.2″	108	TB-H	Reddish	Medium brown	0.11	0.07	0.15	0.34
		TMC18	N 4°34′39.5″	E 9°37′48.9″	108	TB-H	Darkish	Dark grey	− 0.02	− 0.38	− 0.01	− 0.42
	Manjo	TMjo19	N 4°51′45.4″	E 9°50′18.1″	653	AB	Darkish	Medium brown	0.46	− 0.31	0.36	0.51

Table 1 continued

Unit	Location	Sample number	Latitudes	Longitudes	Elevation (m)	Petrography	Apparent colour	Colour	Nitrogen 105 (wt%)	Oxygen 1000 (wt%)	Oxygen 500 (wt%)	Total LOI
Bamileke plateau	Baleng lake	BL30	N 5°32′55.5″	E 10°25′12.4″	1400	B (TB)	Darkish	Light yellow grey	1.89	0.16	1.69	3.75
		BL31	N 5°33′7.4″	E 10°25′33.6″	1374	T (TB)	Reddish	Medium brown	0.82	0.15	0.72	1.69
		BL32	N 5°33′7.4″	E 10°25′33.6″	1374	AB	Darkish	Dark green brown	2.93	− 0.08	1.89	4.74
Noun plain	Noun	N34	N 5°29′17.0″	E 10°34′19.6″	1029	AB	Darkish	Dark yellow grey	3.26	− 0.12	5.36	8.51
		N35	N 5°30′5.1″	E 10°37′6.6″	1056	TB-H	Darkish	Black	0.18	− 0.4	0.04	− 0.19
	Monoun	ML37	N 5°35′21.1″	E 10°35′28.5″	1106	B (TB)	Darkish	Dark yellow grey	0.69	− 0.35	0.34	0.68
		MV38	N 5°36′53.3″	E 10°37′25.9″	1124	B (TB)	Darkish	Med olive	0.16	− 0.5	− 0.02	− 0.35
	Foumbot	FM40	N 5°30′39.3″	E 10°38′55.1″	1073	B (TB)	Darkish	Black	0.61	− 0.49	0.27	0.39
		FM41	N 5°30′39.3″	E 10°39′23.5″	1102	B (TB)	Reddish	Dark yellow brown	0.10	− 0.18	0.19	0.11
		FM42	N 5°30′39.5″	E 10°39′34.7″	1108	B (TB)	Reddish	Dark brown	0.56	− 0.11	0.69	1.13
		FM43	N 5°30′39.5″	E 10°39′34.7″	1108	TB-H	Darkish	Black	0.02	− 0.4	− 0.01	− 0.4
	Mont Mbeppit	ML44	N 5°32′34.9″	E 10°41′55.8″	1374	BTA-M	Darkish	Medium grey	0.00	− 0.37	0.01	− 0.35
		ML45	N 5°32′34.9″	E 10°41′55.8″	1374	TA-B	Reddish	Light green grey	0.28	− 0.22	0.46	0.52
	Koutaba	MB46	N 5°37′47.6″	E 10°37′54.7″	1152	B (TB)	Darkish	Dark grey	− 0.05	− 0.45	− 0.23	− 0.73
		MB47	N 5°37′47.6″	E 10°37′54.7″	1152	B (TB)	Reddish	Dark green grey	0.89	− 0.27	1.09	1.72

BA Basaltic andesite, *AB* Alkaline basalt, *SAB* Sub-alkaline basalt, *TB-H* Trachy-basalt (Hawaiite), *B (TB)* Basanite (Tephrite-Basanite), *T (TB)* Tephrite (TephriteBasanite), *BTA-M* Basaltic Trachy-andesite (Mugearite), *TA-B* Trachy-andesite (Benmoreite). Colours are given in accordance with colour chart after Geo-explore store available in www.goeexplorestore.co.za

on the chemical and mineralogical composition of the pozzolan, the type and proportion of its reactive silica content, and the particle's specific surface area (Pichon 1994; Rodriguez-Camacho and Uribe-Afif 2002; Massazza 2007; Segui 2011).

The aim of this study is to perform a geochemical study while bringing new mineralogical data on pozzolanic outcrops located in the Tombel Plain, Bamileke Plateau, and Noun Plain, three volcanic provinces of the central part of the CVL. X-Ray Diffraction (XRD) analysis allowed making a better comparison and differentiation of the samples by evaluating their mineral (crystal) and non-mineral (amorphous) components. The chemistry of primitive melts from pozzolan clasts helped to understand their petrogenesis as well as making predictions on their pozzolanicity based on ASTM C 618 standard. The comparison of the chemistry of pozzolans with those of nearby volcanoes will help to complete data record on composition of mantle source of magma within the central parts of CVL.

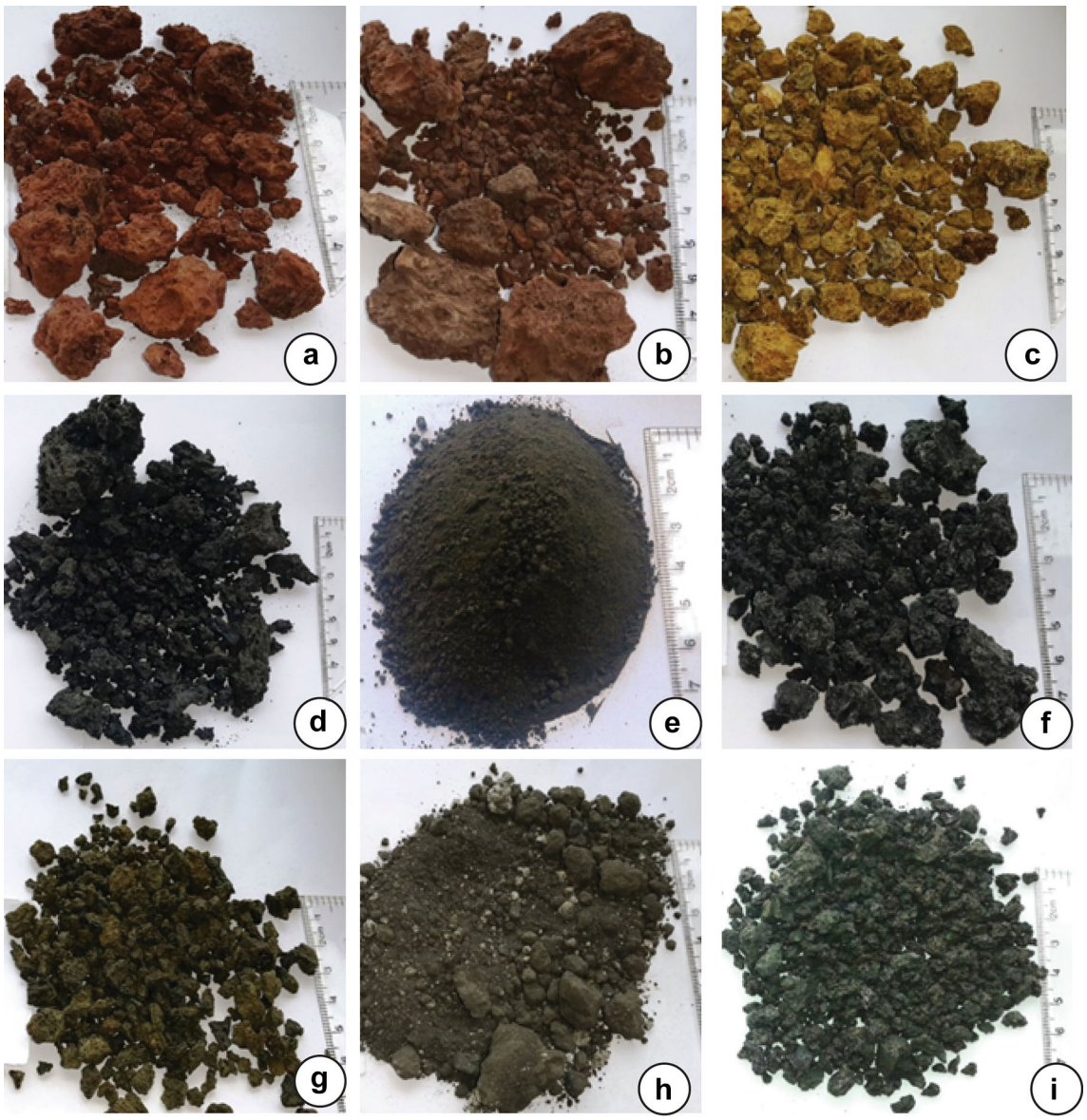

Fig. 3 Pozzolans in hand specimen showing variability in grain sizes and color. **a** Vesiculated medium brown lapilli-ash (Lim52); **b** vesiculated medium brown lapilli-block-ash (TMC17); **c** vesiculated dark green–brown lapilli-ash (BL32); **d** highly—vesiculated black lapilli-block-ash (Lim53); **e** dark green-grey ash-lapilli (Bki48); **f** highly—vesiculated dark grey lapilli-block (TMC18); **g** highly—vesiculated medium olive lapilli-ash pozzolan (MV38); **h** medium olive ash-lapilli (ML44); **i** highly—vesiculated dark grey lapilli-ash (MB46). Colors are in accordance with color chart exhibit in Geo—explore store (www.geoexplorestore.co.za)

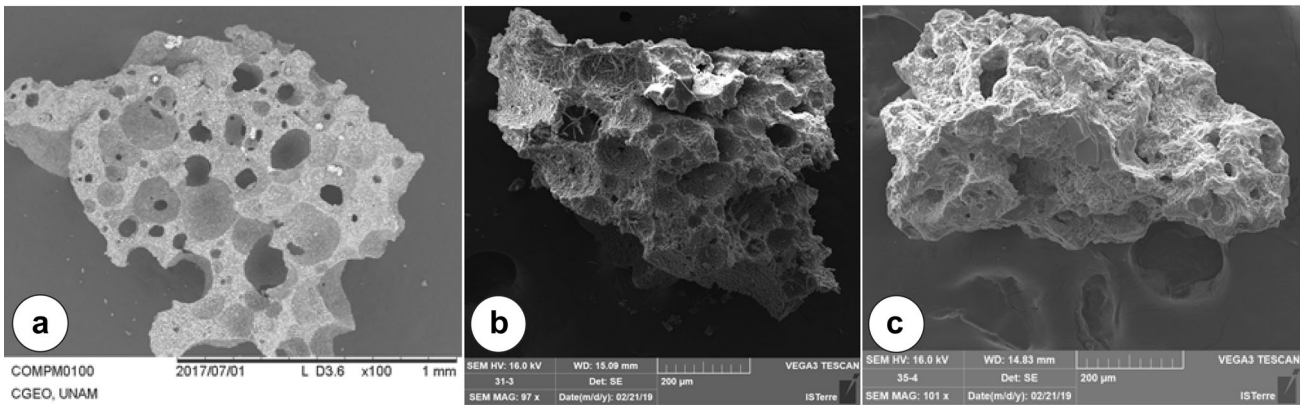

Fig. 4 Scanning Electron Microprobe (SEM) images of the prototype studied pozzolans. **a** Sample Kpé04 from Tombel plain; **b** Sample BL31 from Bamileke Plateau and **c** sample MB46 from Noun Plain. Note overall presence in samples from the three areas of vesicles that evidence degassing while cooling

2 Geological setting

The CVL previously called Cameroon Line (Cantagrel et al. 1978) and renamed as "Cameroon Hot Line" (CHL; Déruelle et al. 2007) defines a SW–NE alignment (trending 30°; Fig. 1) of volcanic massifs and extruded plutons extending on about 1600 km from Pagalù Island in the Gulf of Guinea to Chad Lake (Déruelle et al. 2007). It exhibits the unique worldwide example of an active intraplate volcanic alignment build onto both the oceanic and the continental plates (Fitton and Dunlop 1985; Déruelle et al. 2007). The oceanic part lies within the Gulf of Guinea and comprises the islands of Pagalù, Sao Tomé, Principe, and Bioko (Déruelle et al. 2007). The continental sector is a succession of large polygenetic volcanoes separated by monogenetic volcanic fields, where Hawaiian, strombolian and moderate vulcanian to explosive phreatomagmatic eruptions constructed several short lavas flows, pyroclastic cones and maar volcanoes (Sato et al. 1990; Nkouathio et al. 2008; Chako Tchamabe 2014; Ngwa et al. 2017). The Tombel Plain, Bamileke Plateau, and Noun Plain in the southernmost continental part of the CVL host most of these pyroclastic cones (Figs. 1c, 2). The Tombel plain, for example, displays series of Pleistocene (0.6–0.05 Ma) explosive events (Lee et al. 1994) with about 115 pyroclastics cones of various size (Nkouathio et al. 2006; Tamen et al. 2007) among which mostly consist of black to reddish basaltic pozzolan cones. In the Noun plain, for example, about nine strombolian cones have been recognized as such (Wotchoko et al. 2005; Moundi et al. 2009). The tephra ring of Lake Baleng in the Bamileke Plateau was also evidenced as pozzolans (Wandji et al. 2000). Around the localities of Limbe and Batoke at the foot of Mt Cameroon, some volcanic cones are also made of pozzolans (Bardintzeff and McBirney 2000).

Volcanic rocks from CVL seem to be almost geochemically identical in both ocean and continental sectors. They are dominantly alkali-rich OIB, having similar trends in trace elements (Halliday et al. 1988, 1990; Lee et al. 1994, Déruelle et al. 2007; Asaah et al. 2015). Ballentine et al. (1997) defined a HIMU mantle as the origin of the entire CVL. Fitton and Dunlop (1985) added a metasomatized mantle as part of the source for CVL's lavas. Asaah et al. (2015) provide in a recent review, complementary information on the petrogenetic evolution of the CVL highlighting mantle heterogeneity and distinct geochemical signatures even for individual volcanoes. These lavas form a magmatic series from picrites to rhyolites (Nkouathio et al. 2008), with picrites and alkaline basalts linked to the Noun plain areas (Wotchoko et al. 2005). Lavas from the Tombel Plain, Bamileke Plateau, and Noun Plain provide an opportunity to discuss the petrogenetic evolution of the southernmost continental part of the CVL.

3 Materials and methods

3.1 Fieldwork and sampling

Brief descriptions of the deposits were made onsite and hand specimen collected for further laboratory analyses. Sampling was limited to outcrops, where pozzolans are currently being collected for industrials purposes. Figure 1c and Table 1 present the list of 37 bulk samples collected in the central part of the CVL for mineralogical and geochemical analyses. This includes 22 samples derived from 11 cones of Tombel Plain, 12 samples from five cones in the Noun Plain and three samples from a single cone studied on Bamileke Plateau.

Table 2 Quantitative mineralogy of the Tombel Plain, Bamileke Plateau, and Noun Plain pozzolans

Location	TOMBEL GRABEN/LIMBE										
	Barombi Kotto Island			Limbé Centenarium stadium		Limbé Idenau Junction		Mt Kou pé	On top of Mt Koupé		
Samples	Bki 48	Bki 49	Bki 50	Lim 51	Lim 52	Lim 53	Lim 54	Kpé 02	Kpé 04	Kpé 05	Kpé 06	Kpé 07
Elevation (m)	102	116	105	36	36	167	167	518	813	813	813	654
Olivine (%)		9.4 ± 0.3	6.5 ± 0.3		02.6 ± 0.2	8.30–	9.8–	6.5 ± 0.3	7.1 ± 0.2	13.7 ± 0.4	14.8 ± 0.5	9.3 ± 0.3
Clinopyroxene/Augite	5.3 ± 0.3	54.1 ± 0.9	42.8 ± 0.7	41.6 ± 0.8	37.0 ± 0.5	41.1–	53.0–	27.7 ± 0.5	15.6 ± 0.3	35.1 ± 0.8	21.0 ± 0.9	9.2 ± 0.5
Plagioclase/Anorthite/Labr.	9.4 ± 0.4	25.6 ± 12	37.2 ± 0.8	39.8 ± 1.0	38.2 ± 0.6	22.9–	20.6–	47.4 ± 0.1	23.1 ± 0.5	34.1 ± 0.8	32.6 ± 0.7	28.2 ± 0.4
Orthoclase/Microcline/San			1.3 ± 0.1		9.4 ± 0.3				1.9 ± 0.1			
Albite				3.9 ± 0.1				3.1 ± 0.1				
Nepheline/Leucite			5.6 ± 0.4			5.3–	1.0–		1.1 ± 0.1			
OxidesFe-Ti/Illmémite				2.2 ± 0.2	1.0 ± 0.1							
OxidesFe-Ti/Ti-magnetite	0.6 ± 0.08	5.6 ± 0.2	5.5 ± 0.2					8.1 ± 0.3		0.5 ± 0.1	4.2 ± 0.3	1.4 ± 0.1
OxidesFeIII/Magh_Magnetite							2.4–		0.8 ± 0.1			
OxidesFeII/hematite				8.2 ± 0.2	8.4 ± 0.1		2.9–		3.7 ± 0.1	5.2 ± 0.2		
OxidesFeII + OH/Goethite									0.2 ± 0.1			
OxidesZn.Mn.Fe/Franklinite						7.1–						
Gibbsite				0.9 ± 0.1	1.1 ± 0.1							
Muscovite/Biotite	9.4 ± 0.5	2.5 ± 0.2		2.4 ± 1.0	2.2 ± 0.2			3.6 ± 0.7	1.5 ± 0.3			
Smectite	42.3 ± 1.1											
Fluoroapatite												
Magnesite								0.7 ± 0.1				
Calcite/Portlandite				0.3 ± 0.1								
Quartz	24.3 ± 0.4	0.6 ± 0.1						0.3 ± 0.1	0.8 ± 0.0	1.2 ± 0.2	1.3 ± 0.2	1.0 ± 0.1
Total ± %	91.4	97.7	98.9	99.3	99.9	84.7	89.7	96.8	56.0	89.8	73.9	49.2
Amorphous (%)	8.6 ± 1.7	2.3 ± 1.8	1.1 ± 0.2	0.7 ± 2.0	0 ± 0.0	14.9–	10.2–	2.5 ± 1.5	43.9 ± 0.5	10.1 ± 1.5	26.1 ± 1.5	50.8 ± 0.7
Total (%)	100.0	100.0	100.0	100.0	99.9	99.6	99.9	99.3	99.9	99.9	100.0	100.00
X^2	2.7	2.48	2.79	3.02	2.34	N/A	N/A	2.49	2.03	1.87	1.64	1.88
Rwp (%)	7.85	8.31	8.7	9.17	12.09	N/A	N/A	8.01	7.11	6.82	7.74	6.86

Table 2 continued

Location	LIMBE—TOMBEL GRABEN									
	Tombel town/Loum			Penja	Djombé			Mombo		Manjo
Samples	TL 08	TL 09	TL 10	TPja 13	TDJ 14	TDJ 15	TDJ 16	TMC 17	TMC 18	TMjo 19
Elevation (m)	455	455	455	259	97	97	97	108	108	653
Olivine (%)	8.0 ± 03	7.9 ± 0.3	10.2 ± 0.6	6.4 ± 0.3		6.0 ± 0.4	8.6 ± 0.4	4.4 ± 0.2	7.8 ± 0.3	10.2 ± 0.3
Clinopyroxene/Augite	5.0 ± 0.4	6.3 ± 0.6	10.2 ± 0.5	10.6 ± 0.7	31.6 ± 1.0	25.6 ± 0.7	19.6 ± 0.6	29.4 ± 0.6	25.1 ± 0.5	32.5 ± 0.6
Plagioclase/Anorthite/Labr.	36.5 ± 0.5	40.9 ± 0.7	47.0 ± 0.6	55.6 ± 0.9	41.4 ± 0.2	46.1 ± 0.8	43.4 ± 0.8	45.9 ± 1.0	50.6 ± 0.9	37.6 ± 0.6
Orthoclase/Microcline/San					13.6 ± 0.6	8.1 ± 0.4		2.1 ± 0.2	2.0 ± 0.2	4.5 ± 0.3
Albite					11.5 ± 1.9				2.5 ± 0.1	2.2 ± 0.1
Nepheline/Leucite								6.1 ± 0.4		
OxidesFe-Ti/Illmémite								1.9 ± 0.3		
OxidesFe-Ti/Ti-Magnetite			15.1 ± 0.2	4.2 ± 0.2			3.7 ± 0.7		8.6 ± 0.3	
OxidesFeIII/Magh_Magnetite		4.5 ± 0.2				6.0 ± 0.2	2.9 ± 0.7			3.0 ± 0.2
OxidesFeII/hematite						4.7 ± 0.2		10.4 ± 0.2		7.5 ± 0.2
OxidesFeII + OH/Goethite										
OxidesZn.Mn.Fe/Franklinite										
Gibbsite										
Muscovite/Biotite		5.4 ± 1.0		7.7 ± 0.6						3.0 ± 0.4
Smectite										
Fluoroapatite									1.4 ± 0.2	
Magnesite										
Calcite/Portlandite								0.4 ± 0.0		
Quartz	1.4 ± 0.1	0.5 ± 0.1	1.5 ± 0.1		2.2 ± 0.2	2.5 ± 01	3.3 ± 0.2			0.1 ± 0.0
Total ± %	50.9	65.6	83.7	84.5	100.0	99.0	81.5	100.5	98.1	100.5
Amorphous (%)	49.1 ± 08	34.3 ± 1.4	17.3 ± 1.1	15.5 ± 1.4	− 0.3 ± 2.3	1.1 ± 1.6	18.5 ± 1.4	0.0	1.9 ± 1.3	− 0.5 ± 1.4
Total (%)	100.0	99.92	100.9	100.0	100.3	100.1	100.0	100.0	100.0	100.1
X^2	1.82	1.60	2.07	1.83	6.8	1.96	1.67	2.00	2.48	2.58
Rwp (%)	6.58	7.42	7.08	6.66	13.0	8.35	7.67	6.63	8.00	8.12

Table 2 continued

Location	BAMILEKE PLATEAU			NOUN PLAIN			
	Baleng Lake			Noun		Monoun	
Samples	BL30	BL31	BL32	N34	N35	ML37	MV38
Elevation (m)	1400	1374	1374	1029	1056	1106	1124
Olivine (%)	7.1 ± 0.3	5.1 ± 0.3	8.8 ± 0.2	11.2 ± 0.3	9.9 ± 0.3	16.4 ± 0.4	12.8 ± 0.3
Clinopyroxene/Augite/Diopside	38.5 ± 0.8	36.4 ± 0.7	6.0 ± 0.4	23.44 ± 0.9	25.1 ± 0.5	12.4 ± 0.4	11.1 ± 0.4
Plagioclase/Anorthite/Labr.	22.1 ± 0.5	34.4 ± 1.0	2.5 ± 0.2	19.7 ± 0.3	24.3 ± 0.4	4.1.8 ± 0.2	5.1 ± 0.2
Orthoclase/Microcline/San							
Albite							
Nepheline/Leucite		4.4 ± 0.3			1.9 ± 0.2		
OxidesFe-Ti/Illmémite							
Oxides Fe-Ti/Ti-Magnetite	0.1 ± 0.0				3.9 ± 0.2		0.8 ± 01
Oxides FeIII/Magh_Magnetite	1.6 ± 0.1		1.5 ± 0.1	2.4 ± 0.3		0.7 ± 0.1	0.6 ± 0.1
Oxides FeII/hematite	6.5 ± 0.2	8.0 ± 0.2					
Oxides FeII + OH/Goethite							
Oxides Zn.Mn.Fe/Franklinite				1.8 ± 0.2			
Gibbsite							
Muscovite/Biotite		7.4 ± 04		3.2 ± 0.4	1.7 ± 0.3		
Smectite							
Fluoroapatite							
Magnesite							
Calcite/Portlandite				0.6 ± 0.1	0.5 ± 0.1		
Quartz				1.7 ± 0.1	2.0 ± 0.1	0.7 ± 0.1	0.5 ± 0.1
Total ± %	76.9	95.7	18.9	63.8	69.2	34.4	30.9
Amorphous (%)	23.8 ± 1.2	4.2 ± 0.2	81.2 ± 0.5	36.0 ± 1.0	30.8 ± 1.0	65.6 ± 0.6	69.1 ± 0.6
Total (%)	100.6	99.9	100.1	99.8	100.0	100.0	100.0
X^2	3.27	2.46	2.09	2.48	2.24	2.10	2.16
Rwp (%)	9.23	8.0	7.23	7.9	7.55	7.35	7.51

Table 2 continued

Location	NOUNPLAIN							
	Foumbot Lycée Technique				Mont Mbeppit		Koutaba	
Samples	FM40	FM41	FM42	FM43	ML44	ML45	MB46	MB47
Elevation (m)	1073	1102	1108	1108	1374	1374	1152	1152
Olivine (%)	8.8 ± 0.3	21.1 ± 0.4	15.4 ± 0.4	11.8 ± 0.3	7.1 ± 0.2	6.6 ± 0.3	10.1-	12.7 ± 0.4
Clinopyroxene/Augite/Diopside	26.1 ± 0.5	36.8 ± 0.6	45.9 ± 0.9	32.3 ± 0.6	25.7 ± 0.4	21.0 ± 0.6	24.3-	41.9 ± 0.8
Plagioclase/Anorthite/Labr.	27.0 ± 0.7	21.5 ± 0.4	11.2 ± 0.4	25.7 ± 0.7	11.7 ± 0.5		11.4-	24.3 ± 0.5
Orthoclase/Microcline/San					18.5 ± 0.5	11.8 ± 0.5		
Albite					19.5 ± 0.5	25.1 ± 0.7		
Nepheline/Leucite		3.3 ± 0.3						3.9 ± 0.3
Oxides Fe-Ti/Illmémite					2.6 ± 0.1			
Oxides Fe-Ti/Ti-Magnetite	4.1 ± 0.2			5.2 ± 0.5	5.1 ± 0.1			
Oxides FeIII/Magh_Magnetite		3.1 ± 0.1	6.0 ± 0.3	0.9 ± 0.5		5.8 ± 0.3	1.1-	4.9 ± 0.2
Oxides FeII/hematite		5.2 ± 0.1	1.7 ± 0.2	0.5 ± 0.1				2.0 ± 0.1
Oxides FeII + OH/Goethite								
Oxides Zn.Mn.Fe/Franklinite								
Gibbsite								
Muscovite/Biotite					2.9 ± 0.3	3.2 ± 0.2		
Smectite								
Fluoroapatite		1.7 ± 0.2						
Magnesite								
Calcite/Portlandite			0.2 ± 0.1	0.3 ± 0.1				
Quartz	0.9 ± 0.1			0.7 ± 0.1	6.9 ± 0.2	17.0 ± 0.3		
Total ± %	67.1	92.9	80.5	77.4	100.0	90.5	46.9-	89.7
Amorphous (%)	32.9 ± 1.1	7.1 ± 1.2	19.5 ± 1.3	22.6 ± 1.2	0.0	9.3 ± 1.5	53.20-	10.3 ± 1.4
Total (%)	100.0	100.0	100.0	100.0	100.0	99.8	100.10	100.0
X^2	2.05	2.08	2.20	2.10	1.98	2.10	N/A	2.69
Rwp (%)	7.31	7.47	7.77	7.48	7.59	7.16	N/A	8.63

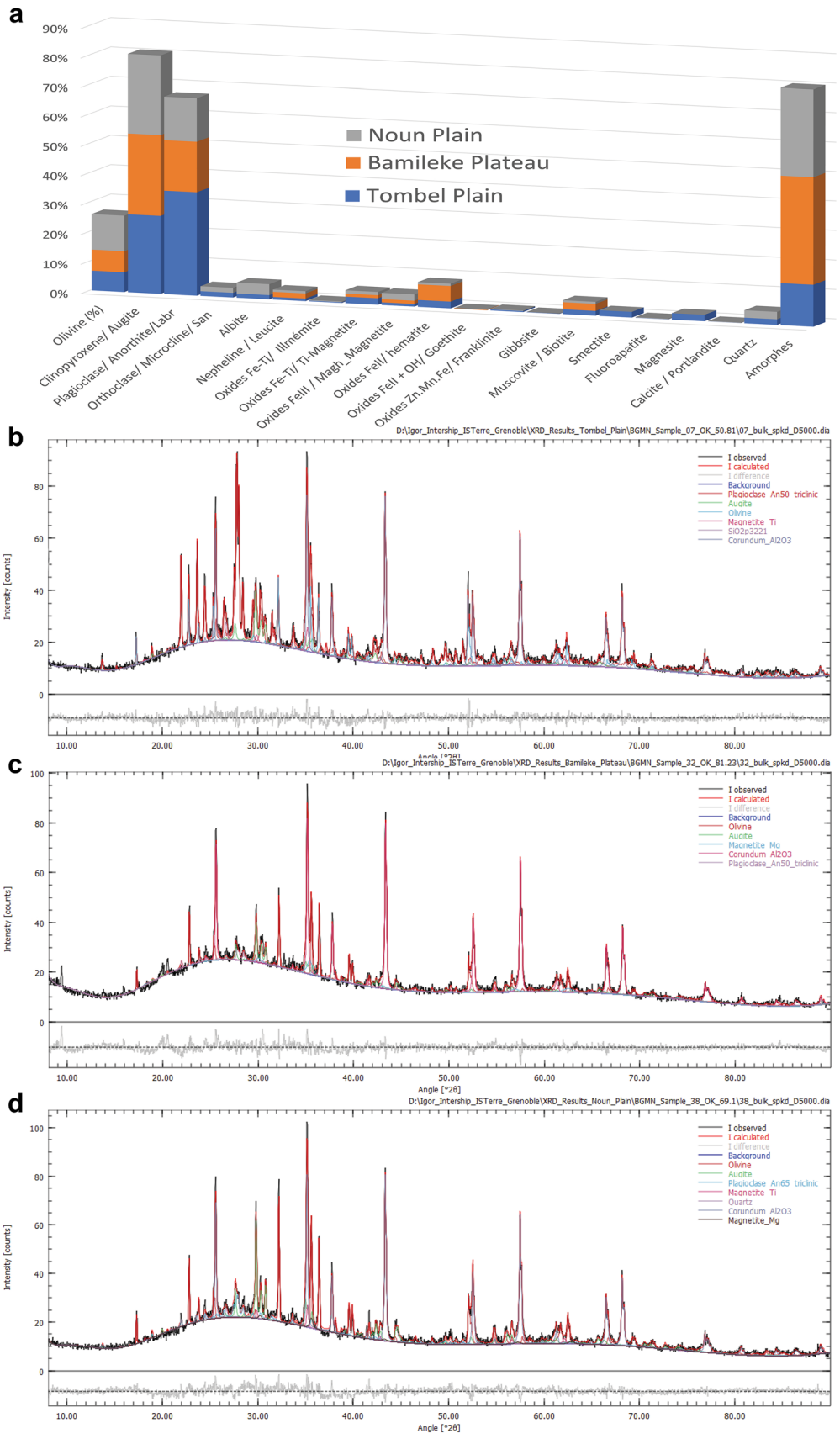
a
90%
80%
70%
60%
50%
40%
30%
20%
10%
0%
Noun Plain
Bamileke Plateau
Tombel Plain
Olivine (%)
Clinopyroxene/ Augite
Plagioclase/ Anorthite/Labr
Orthoclase/ Microcline/ San
Albite
Nepheline / Leucite
Oxides Fe-Ti/ Ilmenite
Oxides Fe-Ti/ Ti-Magnetite
Oxides FeIII / Magh_Magnetite
Oxides FeII/ hematite
Oxides FeII + OH/ Goethite
Oxides Zn.Mn.Fe/ Franklinite
Gibbsite
Muscovite / Biotite
Smectite
Fluoroapatite
Magnesite
Calcite / Portlandite
Quartz
Amorphes
b
D:\Igor_Intership_ISTerre_Grenoble\XRD_Results_Tombel_Plain\BGMN_Sample_07_OK_50.81\07_bulk_spkd_D5000.dia
I observed
I calculated
I difference
Background
Plagioclase An50 triclinic
Augite
Olivine
Magnetite Ti
SiO2a3221
Corundum_Al2O3
Intensity [counts]
10.00
20.00
30.00
40.00
50.00
60.00
70.00
80.00
c
D:\Igor_Intership_ISTerre_Grenoble\XRD_Results_Bamileke_Plateau\BGMN_Sample_32_OK_81.23\32_bulk_spkd_D5000.dia
I observed
I calculated
I difference
Background
Olivine
Augite
Magnetite Mg
Corundum Al2O3
Plagioclase_An50_triclinic
Intensity [counts]
Angle [°2θ]
d
D:\Igor_Intership_ISTerre_Grenoble\XRD_Results_Noun_Plain\BGMN_Sample_38_OK_69.1\38_bulk_spkd_D5000.dia
I observed
I calculated
I difference
Background
Olivine
Augite
Plagioclase An65 triclinic
Magnetite Ti
Quartz
Corundum Al2O3
Magnetite_Mg
Intensity [counts]
Angle [°2θ]

◀**Fig. 5** Quantitative mineralogy of Pozzolans. **a** Average distribution of mineral assemblage and amorphous of the studied pozzolans within the three volcanic fields and Prototypes of XRD patterns of samples **b** Kpe07 from Tombel plain; **c** BL32 from Bamileke plateau and **d** MV38 from Noun plain. See supplementary materials for others analyzed XRD patterns

3.2 Mineralogical analysis

Quantitative mineralogical analyses were performed at the X-Ray Diffractometry Laboratory of the *Institut des Sciences de la Terre (ISTerre)* in Grenoble, France, from X-ray diffraction patterns collected with a Bruker D5000 X-ray diffractometer equipped with a Sol-XE Si(Li) detector from Baltic Scientific Instruments and operated at 40 kV and 40 mA. Juvenile scoria fragments from natural pozzolans field samples carefully selected based on their abundance of vesicles in hand specimen and hand lens observation were first ground in an agate mortar to a powder of 0.315 mm diameter. One gram of this powder was mixed with 20–30 ml of ethanol for 10 min wet grinding in a McCrone micronizing mill containing 48 small cylindrical agate pestles (Hillier 2003). Ethanol was also used to clean the pestle and the mortar and to recover the slurry from the mill. That slurry was dried in an oven for 8 h and smoothly disaggregated using agate mortar. The dry powder was then prepared as a randomly oriented mount and data was recorded from 8 to 90° using 0.026° steps and 16 s counting time per step. XRD data interpretation was performed using the open-access software Profex (3.7.0), which is based on the Rietveld method (Doebelin and Kleeberg 2015), and the American Mineralogist Crystal Structure Database that contains XRD data for known minerals (www.rruff.geo.arizona.edu). Each sample was run twice using 400–800 mg of the powdered rock. The first pattern was used for phase identification and quantitative phase analysis of crystalline phases, whereas the second pattern, collected after addition of 20 wt% of an Al_2O_3 (corundum) internal standard, was used to quantify the amorphous component of samples (Jenkins and Snyder 1996; Madsen et al. 2011; Raven and Self 2017). The rare occurrence and limited variety of clay minerals allowed their identification and quantification, using XRD patterns obtained from randomly oriented powders.

3.3 Major and trace elements analysis

Representative fresh coarse lapilli to bomb sizes pozzolans collected from the deposits were prepared and analyzed at the GEOLAB (Ontario, Canada) for their major and trace element abundances following the laboratory techniques and methods (Geoscience Laboratories 2015). Special care was taken to select only the freshest core/parts of the samples for the analyses.

Loss on ignition (LOI) was performed by calcinating about 20 g of the sample at 105 °C under a nitrogen atmosphere then, at 500 and 1000 °C under an oxygen atmosphere. The results were represented in percentage, and the reduction of weight noticed after calcination compared to the weight of the fresh sample.

Major elements were determined by X-Ray Fluorescence (XRF) by fusing 10 grams of the burned samples with a borate flux to produce a glass bead for the analysis. Trace elements were determined by Inductively Coupled Plasma Mass Spectrometry (ICP-MS). Sample preparation involved Agate Mill Preparation (SAM-AGM) techniques to reduce the size of rock particles to less than 90 µm (170 Mesh). The use of this method reduces the amount of contamination by Cr, Al, and Fe. Then, the Closed Vessel Multi-Acid Digest (SOL-CAIO) method (Geoscience Laboratories 2015) was used for the complete dissolution of the silicate rock sample. Finally, prepared solutions were analyzed by ICP-MS and ICP-AES to determine their composition in trace elements. Ferrous irons were quantified by potentiometric titration with a standardized permanganate solution to bring more accurate data in iron determination. For that purpose, samples were first dissolved in an aggressive non-oxidizing acid mix. On the other hand, measurements of geochemical standards (DUP: Laboratory Duplicate) were carried out to guarantee the quality and accuracy of the analyses. The CIPW norm was determined using the GCD kit (Janousek et al. 2006).

4 Results

4.1 Petrography

The pozzolan deposits consist of pyroclastic materials that slightly differed on outcrops by some physical characteristics such as grain size, color, and vesicle abundance (Table 1, Figs. 2, 3, 4). In the Tombel Plain and Bamileke Plateau, pozzolans deposits are exposed in the form of large cones, very often well-stratified and graded (Fig. 2a, b), while those in the Noun Plain appear either as small cones (Fig. 2c, d) or large sub-horizontal expanses without any apparent grading (Fig. 2e). In hand-samples, the pozzolans consist of a mixture of grains with sizes varying from blocks ($\phi > 64$ mm) to ash ($\phi < 2$ mm). Lapilli is the dominant component. The color of pozzolans also varies from brownish to darkish (Table 1, Fig. 3), and most samples show vesicles (Figs. 3a–c, 4).

Table 3 Geochemical and CIPW composition of Tombel Plain, Bamileke Plateau and Noun Plain pozzolans

Samples	Bki48 Tombel Plain	Bki49	Bki50	Lim51	Lim52	Lim53	Lim54	Kpé02	Kpé04	Kpé05	Kpé06
Lithology	BA	AB	AB	AB	AB	AB	AB	AB	AB	AB	AB
SiO_2 (Wt %)	55.02	45.98	46.27	46.45	46.63	44.83	44.71	45.47	45.17	45.03	44.78
TiO_2	2.23	2.86	2.87	3.20	3.16	2.91	2.90	3.31	2.99	3.25	3.25
Al_2O_3	17.63	14.36	14.62	14.36	14.27	12.13	12.08	15.33	14.24	14.46	14.47
Fe_2O_3	6.87	5.14	4.99	12.99	12.51	4.39	5.25	5.86	11.72	10.62	6.54
FeO	3.57	6.46	6.48	0.17	0.37	7.72	7.09	7.55	1.95	3.42	6.89
Fe_2O_3 (T)	10.85	12.32	12.19	13.19	12.92	12.97	13.14	14.25	13.89	14.41	14.20
MgO	4.42	7.87	7.64	6.42	6.73	9.74	10.38	7.43	8.41	9.17	8.87
MnO	0.13	0.20	0.19	0.19	0.19	0.20	0.20	0.19	0.19	0.20	0.20
BaO	0.04	0.05	0.05	0.04	0.05	0.04	0.03	0.04	0.04	0.04	0.05
CaO	6.16	11.31	11.27	10.85	11.00	13.06	13.01	9.37	10.09	9.72	9.94
Na_2O	1.60	3.18	3.09	3.37	3.28	2.59	2.13	3.05	3.17	2.13	2.35
K_2O	1.49	1.37	1.30	1.39	1.20	1.04	0.93	1.08	1.18	0.95	1.22
Cr_2O_3	0.03	0.05	0.04	0.05	0.05	0.07	0.08	0.02	0.03	0.04	0.04
P_2O_5	0.38	0.48	0.48	0.52	0.52	0.42	0.42	0.46	0.58	0.59	0.62
Total	100.00	100.00	100.00	100.00	100.00	100.00	100.00	100.00	100.00	100.00	100.00
Mg#	55.28	54.90	54.13	97.39	94.74	55.77	59.40	49.59	81.15	72.86	56.29
Q	21.30	0.00	0.00	0.00	0.00	0.00	0.00	0.00	0.00	0.00	0.00
C	3.10	0.00	0.00	0.00	0.00	0.00	0.00	0.00	0.00	0.00	0.00
Or	8.81	8.07	7.67	8.19	7.11	6.14	5.50	6.41	7.00	5.64	7.22
Ab	13.55	18.74	20.43	28.49	27.72	11.14	13.24	25.81	25.42	18.01	19.90
An	28.06	20.90	22.21	19.97	20.67	18.39	20.64	24.94	21.14	27.08	25.32
Ne	0.00	4.40	3.09	0.00	0.00	5.84	2.60	0.00	0.76	0.00	0.00
Di	0.00	25.35	24.18	16.12	16.88	34.76	32.56	14.73	17.90	13.43	15.65
Hy	11.01	0.00	0.00	0.00	0.32	0.00	0.00	1.31	0.00	16.30	6.57
Ol	0.00	7.74	7.83	5.97	6.05	9.89	10.48	10.06	8.87	0.23	7.39
Mt	5.48	7.45	7.24	0.00	0.00	6.37	7.62	8.50	0.00	2.24	9.49
Il	4.23	5.44	5.45	0.77	1.19	5.54	5.51	6.30	4.54	6.18	6.17
Hm	3.09	0.00	0.00	13.00	12.51	0.00	0.00	0.00	11.72	9.07	0.00
Tn	0.00	0.00	0.00	4.72	6.23	0.00	0.00	0.00	0.00	0.00	0.00
Pf	0.00	0.00	0.00	1.48	0.00	0.00	0.00	0.00	1.02	0.00	0.00
Ap	0.90	1.14	1.15	1.23	1.23	1.00	1.00	1.08	1.38	1.40	1.48
Sum	99.53	99.23	99.24	99.94	99.89	99.06	99.14	99.13	99.74	99.57	99.18

Table 3 continued

Samples	Bki48 Tombel Plain	Bki49	Bki50	Lim51	Lim52	Lim53	Lim54	Kpé02	Kpé04	Kpé05	Kpé06
Lithology	BA	AB	AB	AB	AB	AB	AB	AB	AB	AB	AB
DI	74.82	52.11	53.40	56.65	55.50	41.51	41.97	57.16	54.32	50.72	52.44
Ti (in ppm)	12,365.00	17,064.00	17033.00	19,043.00	18,705.00	17,562.00	17,367.00	19,867.00	17,731.00	18,987.00	19,269.00
Rb	45.06	36.46	35.24	29.81	22.76	23.18	20.10	21.63	25.76	27.04	30.87
Cs	1.62	0.59	0.56	0.29	0.21	0.35	0.26	0.20	0.31	0.33	0.35
Sr	441.60	858.90	872.40	820.10	830.70	698.20	685.10	644.00	674.40	687.60	743.30
Ba	388.30	429.00	441.70	414.10	406.10	323.60	312.10	339.00	377.40	415.40	437.30
Sc	22.00	27.60	26.70	27.30	27.30	36.10	35.50	25.40	24.30	26.50	25.40
V	227.20	288.30	287.00	255.20	277.50	328.00	316.20	278.40	232.10	255.20	269.90
Cr	227.00	328.00	279.00	322.00	328.00	505.00	523.00	172.00	245.00	271.00	222.00
Co	33.52	46.99	45.73	49.07	46.96	55.44	57.33	53.47	55.04	56.18	55.62
Ni	83.50	123.20	114.10	138.20	165.20	165.70	187.20	122.70	167.20	151.10	147.40
Zn	113.00	108.00	107.00	119.00	117.00	103.00	102.00	120.00	116.00	113.00	112.00
Zr	261.00	304.00	314.00	335.00	331.00	245.00	240.00	234.00	236.00	249.00	254.00
Nb	59.68	80.29	83.45	78.20	77.51	61.92	60.51	46.31	55.78	63.08	65.24
Hf	6.19	6.89	7.08	7.55	7.50	5.88	5.64	5.85	5.50	5.79	5.91
Ta	3.77	4.94	5.12	4.96	4.88	3.91	3.80	2.84	3.35	3.77	3.91
Pb	12.20	3.30	1.40	4.60	4.30	2.80	2.80	1.20	5.20	2.20	2.20
Th	11.00	7.18	7.38	7.35	7.24	4.83	4.62	2.80	3.63	4.14	4.26
U	2.90	1.83	1.96	1.64	1.83	1.36	1.30	0.78	1.03	1.02	1.15
Y	26.94	28.25	27.74	28.67	28.61	23.66	23.14	30.26	28.39	28.99	29.28
La (in ppm)	60.42	62.39	64.08	61.36	60.74	47.25	45.67	29.90	38.46	41.98	42.82
Ce	121.48	123.14	126.15	124.99	123.36	99.11	96.43	64.49	78.58	85.77	86.89
Pr	14.01	14.40	14.78	14.87	14.71	12.21	11.73	8.29	9.95	10.68	10.91
Nd	53.03	54.53	55.93	58.30	57.81	48.82	46.74	36.02	40.55	43.56	44.72
Sm	9.23	9.61	9.81	10.46	10.52	8.85	8.35	8.05	8.35	8.86	8.97
Eu	2.51	2.92	2.97	3.19	3.16	2.67	2.58	2.71	2.73	2.86	2.90
Gd	7.41	7.80	7.85	8.55	8.35	7.05	6.77	7.82	7.49	8.08	8.01
Tb	1.02	1.07	1.07	1.14	1.14	0.93	0.91	1.11	1.05	1.09	1.11
Dy	5.64	5.92	5.95	6.19	6.08	5.10	4.94	6.32	5.85	6.07	6.19
Ho	1.02	1.03	1.04	1.08	1.07	0.88	0.87	1.14	1.04	1.07	1.08
Er	2.71	2.73	2.73	2.77	2.73	2.29	2.20	2.86	2.71	2.74	2.78
Tm	0.37	0.36	0.36	0.35	0.36	0.30	0.29	0.37	0.35	0.35	0.35
Yb	2.27	2.14	2.15	2.12	2.08	1.78	1.75	2.20	2.02	2.05	2.07

Table 3 continued

Samples	Bki48 Tombel Plain	Bki49	Bki50	Lim51	Lim52	Lim53	Lim54	Kpé02	Kpé04	Kpé05	Kpé06
Lithology	BA	AB	AB	AB	AB	AB	AB	AB	AB	AB	AB
Lu	0.32	0.31	0.31	0.30	0.30	0.25	0.24	0.31	0.28	0.29	0.29
La/Yb	26.68	29.18	29.79	28.92	29.24	26.49	26.11	13.59	19.06	20.46	20.69
Zr/Nb	4.37	3.79	3.77	4.28	4.27	3.96	3.97	5.05	4.23	3.95	3.89
Nb/U	20.59	43.90	42.62	47.60	42.29	45.39	46.58	59.21	54.10	61.66	56.93
La/Nb	1.01	0.78	0.77	0.78	0.78	0.76	0.75	0.65	0.69	0.67	0.66
Ba/Nb	6.51	5.34	5.29	5.30	5.24	5.23	5.16	7.32	6.77	6.59	6.70
(La/Yb)N	17.84	19.51	19.92	19.34	19.56	17.71	17.46	9.09	12.74	13.68	13.83
Th/Yb	4.86	3.36	3.43	3.46	3.49	2.71	2.64	1.27	1.80	2.02	2.06
Nb/Yb	26.35	37.55	38.80	36.85	37.32	34.71	34.60	21.05	27.64	30.74	31.52
Samples	Kpé07 Tombel Plain	TL08	TL09	TL10	TPja13	TDJ14	TDJ15	TDJ16	TMC17	TMC18	TMjo19
Lithology	SAB	SAB	SAB	AB	AB	TB-H	TB-H	TB-H	TB-H	TB-H	AB
SiO_2 (wt%)	47.55	49.41	49.59	48.81	47.37	49.86	48.75	47.71	46.30	46.05	45.04
TiO_2	2.91	2.90	3.02	2.89	2.69	2.66	2.73	2.95	2.82	2.89	3.22
Al_2O_3	14.13	15.63	16.17	15.46	19.44	15.47	15.55	16.16	15.36	15.34	14.90
Fe_2O_3	3.34	4.93	6.54	4.05	8.39	6.22	9.47	5.42	13.14	5.72	8.32
FeO	9.35	7.60	6.44	8.09	5.22	5.71	3.06	7.31	0.13	7.10	5.21
Fe_2O_3 (T)	13.73	13.37	13.70	13.04	14.19	12.56	12.87	13.55	13.28	13.61	14.11
MgO	7.82	6.49	5.94	6.41	3.88	4.88	5.05	5.22	7.12	7.23	7.72
MnO	0.17	0.17	0.17	0.17	0.26	0.20	0.20	0.21	0.19	0.19	0.20
BaO	0.03	0.03	0.03	0.03	0.10	0.07	0.07	0.07	0.05	0.05	0.05
CaO	9.45	7.94	7.58	8.43	6.80	7.55	7.93	8.16	9.08	8.87	9.33
Na_2O	3.00	2.85	2.59	3.24	3.28	3.86	3.94	3.31	3.80	3.78	3.20
K_2O	0.84	0.77	0.80	1.03	1.01	2.10	2.09	1.86	1.38	1.39	1.49
Cr_2O_3	0.03	0.03	0.02	0.02	0.00	0.00	0.00	0.00	0.02	0.02	0.02
P_2O_5	0.35	0.39	0.39	0.47	0.98	0.79	0.81	0.78	0.62	0.58	0.72
Total	100.00	100.00	100.00	100.00	100.00	100.00	100.00	100.00	100.00	100.00	100.00
Mg#	45.53	46.07	48.01	44.20	42.67	46.07	62.25	41.63	98.20	50.45	59.74
Q	0.00	3.83	7.73	0.00	6.82	0.50	0.00	0.00	0.00	0.00	0.00
C	0.00	0.00	0.00	0.00	2.93	0.00	0.00	0.00	0.00	0.00	0.00
Or	4.98	4.57	4.74	6.08	5.98	12.39	12.34	11.00	8.15	8.24	8.81

Table 3 continued

Samples	Kpé07 Tombel Plain	TL08	TL09	TL10	TPja13	TDJ14	TDJ15	TDJ16	TMC17	TMC18	TMjo19
Lithology	SAB	SAB	SAB	AB	AB	TB-H	TB-H	TB-H	TB-H	TB-H	AB
Ab	25.38	24.14	21.89	27.40	27.77	32.69	33.31	28.03	32.19	25.87	25.20
An	22.59	27.56	30.13	24.61	27.33	18.68	18.60	23.73	20.75	20.76	21.87
Ne	0.00	0.00	0.00	0.00	0.00	0.00	0.00	0.00	0.00	3.33	1.03
Di	17.86	7.41	3.90	11.39	0.00	10.70	12.00	9.33	9.10	15.43	15.33
Hy	6.90	18.01	14.73	16.09	9.68	8.45	3.59	8.54	0.00	0.00	0.00
Ol	10.03	0.00	0.00	1.02	0.00	0.00	2.41	3.20	9.48	10.40	8.51
Mt	4.85	7.15	9.49	5.87	9.85	9.02	2.62	7.86	0.00	8.30	8.10
Il	5.53	5.52	5.73	5.50	5.11	5.05	5.19	5.61	0.68	5.49	6.12
Hm	0.00	0.00	0.00	0.00	1.60	0.00	7.67	0.00	13.14	0.00	2.74
Tn	0.00	0.00	0.00	0.00	0.00	0.00	0.00	0.00	2.75	0.00	0.00
Pf	0.00	0.00	0.00	0.00	0.00	0.00	0.00	0.00	2.28	0.00	0.00
Ap	0.82	0.93	0.93	1.12	2.31	1.87	1.93	1.86	1.46	1.38	1.71
Sum	98.94	99.12	99.26	99.08	99.39	99.34	99.64	99.16	99.97	99.19	99.41
DI	52.95	60.10	64.49	58.09	70.83	64.26	64.25	62.76	61.09	58.20	56.90
Ti (in ppm)	17,485.00	17,705.00	17,126.00	17,384.00	15,099.00	15,948.00	15,958.00	17,431.00	16,768.00	17,308.00	19,376.00
Rb	16.42	15.73	17.79	20.20	30.34	67.63	64.48	68.57	36.62	32.89	35.60
Cs	0.17	0.16	0.19	0.22	0.82	1.40	1.36	0.94	0.31	0.37	0.39
Sr	473.80	528.50	536.10	574.00	1090.90	856.80	860.10	937.40	745.80	704.70	834.90
Ba	253.90	268.60	280.80	315.20	855.70	647.80	649.60	643.50	454.60	426.70	513.30
Sc	25.40	21.40	20.30	20.20	12.70	14.50	14.70	15.80	20.50	19.50	21.70
V	253.50	184.40	164.40	198.90	137.30	199.70	202.40	210.60	206.80	226.90	259.60
Cr	224.00	217.00	171.00	158.00	9.00	18.00	21.00	20.00	144.00	114.00	132.00
Co	53.91	48.80	45.85	44.93	32.25	35.52	35.64	38.11	46.72	47.97	50.96
Ni	150.40	123.70	106.00	95.20	17.10	21.60	21.60	24.90	105.40	102.30	114.20
Zn	112.00	114.00	110.00	112.00	153.00	120.00	118.00	123.00	116.00	126.00	123.00
Zr	168.00	186.00	186.00	205.00	496.00	350.00	350.00	370.00	275.00	260.00	333.00
Nb	33.79	37.67	36.85	42.86	123.48	91.71	91.94	98.44	65.25	62.56	82.87
Hf	4.41	4.66	4.82	5.07	10.41	7.71	7.86	7.93	6.42	6.03	7.42
Ta	2.08	2.23	2.29	2.57	7.73	5.67	5.86	5.94	3.98	3.80	5.10
Pb	1.20	1.30	1.30	1.60	5.50	6.60	6.50	5.00	2.30	2.80	2.80
Th	2.00	2.13	2.23	2.57	10.31	8.43	8.11	8.00	5.02	4.52	6.04

Table 3 continued

Samples	Kpé07 Tombel Plain	TL08	TL09	TL10	TPja13	TDJ14	TDJ15	TDJ16	TMC17	TMC18	TMjo19
Lithology	SAB	SAB	SAB	AB	AB	TB-H	TB-H	TB-H	TB-H	TB-H	AB
U	0.56	0.58	0.63	0.72	2.47	2.20	2.36	2.06	1.28	1.13	1.64
Y	27.78	27.85	27.87	28.38	38.54	30.86	31.51	32.46	28.68	27.30	31.44
La (in ppm)	21.46	23.26	24.27	27.67	90.20	65.44	65.51	66.92	47.09	43.56	56.76
Ce	47.20	50.94	53.14	59.29	176.39	128.57	126.63	132.00	94.62	87.24	115.00
Pr	6.17	6.82	7.12	7.77	20.03	15.13	14.86	15.43	11.35	10.41	13.68
Nd	27.49	30.41	31.16	33.76	73.50	57.59	57.62	58.86	45.41	42.17	53.91
Sm	6.50	6.92	7.24	7.47	12.78	10.35	10.40	10.62	8.74	8.21	10.12
Eu	2.27	2.43	2.53	2.59	3.99	3.13	3.19	3.27	2.82	2.66	3.19
Gd	6.79	6.91	7.23	7.30	10.45	8.58	8.75	8.94	7.73	7.42	8.70
Tb	0.99	1.00	1.03	1.03	1.42	1.16	1.21	1.21	1.07	1.04	1.20
Dy	5.73	5.61	5.80	5.90	7.76	6.48	6.72	6.62	5.96	5.76	6.62
Ho	1.04	1.01	1.02	1.04	1.39	1.17	1.18	1.16	1.05	1.03	1.16
Er	2.65	2.56	2.69	2.69	3.68	3.03	3.11	3.14	2.73	2.59	3.00
Tm	0.34	0.33	0.35	0.35	0.49	0.41	0.41	0.41	0.35	0.33	0.39
Yb	2.04	1.98	2.06	2.02	2.99	2.41	2.50	2.52	2.13	2.00	2.29
Lu	0.28	0.28	0.29	0.29	0.43	0.35	0.36	0.36	0.30	0.28	0.33
La/Yb	10.51	11.75	11.79	13.67	30.20	27.20	26.18	26.60	22.10	21.77	24.79
Zr/Nb	4.97	4.94	5.05	4.78	4.02	3.82	3.81	3.76	4.21	4.16	4.02
Nb/U	60.01	65.06	58.49	59.37	50.01	41.72	38.96	47.83	50.98	55.37	50.68
La/Nb	0.64	0.62	0.66	0.65	0.73	0.71	0.71	0.68	0.72	0.70	0.68
Ba/Nb	7.51	7.13	7.62	7.35	6.93	7.06	7.07	6.54	6.97	6.82	6.19
(La/Yb)N	7.03	7.86	7.88	9.14	20.19	18.19	17.51	17.79	14.78	14.56	16.57
Th/Yb	0.98	1.08	1.08	1.27	3.45	3.50	3.24	3.18	2.36	2.26	2.64
Nb/Yb	16.55	19.03	17.90	21.18	41.34	38.12	36.75	39.12	30.62	31.27	36.19

Samples	BL30 Bamileke Plateau	BL31	BL32	N34 Noun Plain	N35	ML37
Lithology	B(TB)	T(TB)	AB	AB	TB-H	B(TB)
SiO_2	42.20	43.33	45.10	46.20	46.41	43.55
TiO_2	3.34	3.22	3.26	2.98	2.78	2.71
Al_2O_3	15.09	14.45	14.59	15.83	14.28	12.87
Fe_2O_3	13.05	12.49	9.46	5.87	3.99	3.22
FeO	1.45	1.34	4.27	7.12	7.87	9.11

Table 3 continued

Samples	BL30 Bamileke Plateau	BL31	BL32	N34 Noun Plain	N35	ML37
Lithology	B(TB)	T(TB)	AB	AB	TB-H	B(TB)
Fe_2O_3(T)	14.66	13.98	14.20	13.79	12.74	13.34
MgO	8.96	8.29	8.77	8.04	8.16	12.21
MnO	0.21	0.20	0.21	0.20	0.19	0.20
BaO	0.08	0.07	0.07	0.07	0.07	0.06
CaO	10.75	11.03	9.59	8.42	9.62	9.75
Na_2O	2.83	3.22	2.16	2.53	3.54	3.24
K_2O	1.11	1.50	1.39	1.28	1.58	1.36
Cr_2O_3	0.03	0.03	0.03	0.03	0.04	0.05
P_2O_5	0.72	0.67	0.63	0.63	0.60	0.64
Total	100.00	100.00	100.00	100.00	100.00	100.00
Mg#	86.09	86.09	67.26	53.02	50.91	57.27
Q	0.00	0.00	0.00	0.00	0.00	0.00
C	0.00	0.00	0.00	0.00	0.00	0.00
Or	6.59	8.88	8.20	7.54	9.33	8.06
Ab	19.58	18.16	18.28	21.42	21.08	9.95
An	25.15	20.53	26.02	28.06	18.41	16.53
Ne	2.38	4.93	0.00	0.00	4.81	9.48
Di	14.23	19.14	13.55	7.61	20.36	22.19
Hy	0.00	0.00	12.75	15.73	0.00	0.00
Ol	11.02	8.26	1.97	3.11	12.59	21.39
Mt	0.00	0.00	4.98	8.52	5.79	4.67
Il	3.52	3.27	6.20	5.66	5.27	5.14
Hm	13.05	12.49	6.03	0.00	0.00	0.00
Tn	0.00	0.00	0.00	0.00	0.00	0.00
Pf	2.54	2.56	0.00	0.00	0.00	0.00
Ap	1.70	1.59	1.50	1.48	1.42	1.51
Sum	99.77	99.80	99.48	99.13	99.06	98.91
DI	53.70	52.50	52.50	57.02	53.63	44.02
Ti (in ppm)	19,471.00	18,464.00	18,958.00	16,556.00	16,907.00	16,173.00
Rb	25.94	30.80	34.97	37.21	39.36	31.19
Cs	0.39	0.37	0.51	0.74	0.41	0.34
Sr	933.80	858.00	971.80	653.90	830.00	739.50
Ba	704.60	611.30	712.60	585.90	652.50	533.60

Table 3 continued

Samples	BL30 Bamileke Plateau	BL31	BL32	N34 Noun Plain	N35	ML37
Lithology	B(TB)	T(TB)	AB	AB	TB-H	B(TB)
Sc	25.20	25.00	25.30	22.50	23.80	23.40
V	221.40	245.70	232.40	212.00	224.60	228.60
Cr	192.00	210.00	193.00	221.00	247.00	341.00
Co	54.58	51.16	52.91	47.52	47.72	59.16
Ni	137.80	124.30	132.50	126.20	125.70	298.40
Zn	113.00	98.00	100.00	93.00	102.00	101.00
Zr	257.00	237.00	237.00	243.00	241.00	239.00
Nb	87.20	81.03	83.06	69.03	72.05	72.39
Hf	5.68	5.61	5.31	5.67	5.44	5.35
Ta	4.89	4.83	4.70	4.07	4.19	4.29
Pb	3.40	4.30	2.50	6.40	3.70	2.20
Th	5.73	6.28	5.82	7.55	6.16	5.06
U	1.41	1.58	1.41	1.64	1.29	1.30
Y	26.75	26.42	26.37	26.14	26.02	24.89
La	57.68	56.47	55.07	55.02	53.35	48.02
Ce	106.11	108.20	105.91	108.52	101.91	91.93
Pr	12.81	12.49	12.16	12.45	11.99	10.92
Nd	50.67	49.04	47.57	48.92	46.97	43.59
Sm	9.11	9.06	8.86	9.03	8.67	8.32
Eu	3.18	3.01	2.96	2.95	3.02	2.79
Gd	7.79	7.78	7.58	7.58	7.65	7.30
Tb	1.04	1.05	1.02	1.02	1.02	0.98
Dy	5.61	5.79	5.53	5.60	5.59	5.35
Ho	0.99	1.01	0.99	0.98	0.97	0.95
Er	2.55	2.62	2.51	2.54	2.49	2.38
Tm	0.32	0.34	0.33	0.33	0.32	0.31
Yb	1.91	1.98	1.93	1.95	1.90	1.80
Lu	0.28	0.29	0.27	0.28	0.26	0.26
La/Yb	30.21	28.53	28.47	28.17	28.14	26.68
Zr/Nb	2.95	2.92	2.85	3.52	3.35	3.30
Nb/U	61.89	51.25	59.03	42.09	55.72	55.51
La/Nb	0.66	0.70	0.66	0.80	0.74	0.66
Ba/Nb	8.08	7.54	8.58	8.49	9.06	7.37

Table 3 continued

Samples	BL30 Bamileke Plateau	BL31	BL32	N34 Noun Plain	N35	ML37
Lithology	B(TB)	T(TB)	AB	AB	TB-H	B(TB)
(La/Yb)N	20.20	19.08	19.04	18.84	18.82	17.84
Th/Yb	3.00	3.17	3.01	3.86	3.25	2.81
Nb/Yb	45.68	40.95	42.95	35.34	38.00	40.22

Samples	MV38 Noun Plain	FM40	FM41	FM42	FM43	ML44	ML45	MB46	MB47
Lithology	B(TB)	B(TB)	B(TB)	B(TB)	TB-H	BTA-M	TA-B	B(TB)	B(TB)
SiO_2	43.81	45.20	43.21	43.59	43.85	54.34	57.38	43.80	43.48
TiO_2	2.77	3.00	2.60	2.97	2.56	2.09	1.89	2.75	2.99
Al_2O_3	13.27	14.42	11.99	13.36	12.56	13.51	13.44	13.50	13.62
Fe_2O_3	2.92	3.82	9.20	8.38	3.92	4.50	4.63	3.75	7.87
FeO	9.27	8.62	3.69	4.58	8.31	5.07	4.44	9.22	5.04
Fe_2O_3(T)	13.22	13.40	13.30	13.47	13.16	10.14	9.56	14.00	13.47
MgO	10.68	8.24	13.77	10.38	12.83	6.24	5.40	10.32	10.45
MnO	0.20	0.20	0.19	0.20	0.20	0.16	0.15	0.22	0.20
BaO	0.06	0.07	0.06	0.06	0.07	0.05	0.05	0.06	0.07
CaO	10.30	9.78	9.21	10.21	9.12	6.89	5.65	9.67	10.87
Na_2O	3.53	3.50	3.48	3.39	3.44	3.60	3.33	3.63	2.73
K_2O	1.47	1.52	1.52	1.66	1.52	2.52	2.71	1.45	1.36
Cr_2O_3	0.04	0.04	0.05	0.04	0.05	0.02	0.02	0.04	0.06
P_2O_5	0.63	0.65	0.61	0.67	0.63	0.44	0.42	0.58	0.69
Total	100.00	100.00	100.00	100.00	100.00	100.00	100.00	100.00	100.00
Mg#	53.54	48.87	78.86	69.38	60.68	55.15	54.87	52.80	67.48
Q	0.00	0.00	0.00	0.00	0.00	3.73	10.49	0.00	0.00
C	0.00	0.00	0.00	0.00	0.00	0.00	0.00	0.00	0.00
Or	8.70	8.98	8.97	9.79	9.00	14.91	16.00	8.58	8.03
Ab	8.85	17.91	12.08	13.48	11.05	30.45	28.20	11.40	15.16
An	16.01	19.14	12.60	16.33	14.36	13.25	13.72	16.25	20.91
Ne	11.41	6.35	9.41	8.25	9.77	0.00	0.00	10.47	4.30
Di	24.92	20.23	22.63	23.33	21.33	14.25	9.10	22.49	22.17
Hy	0.00	0.00	0.00	0.00	0.00	11.26	10.69	0.00	0.00
Ol	18.04	13.62	16.68	10.53	21.45	0.00	0.00	17.72	11.05
Mt	4.24	5.54	4.98	6.78	5.69	6.53	6.71	5.44	8.22

Table 3 continued

Samples	MV38 Noun Plain	FM40	FM41	FM42	FM43	ML44	ML45	MB46	MB47
Lithology	B(TB)	B(TB)	B(TB)	B(TB)	TB-H	BTA-M	TA-B	B(TB)	B(TB)
Il	5.27	5.70	4.95	5.65	4.87	3.98	3.59	5.22	5.69
Hm	0.00	0.00	5.77	3.71	0.00	0.00	0.00	0.00	2.20
Tn	0.00	0.00	0.00	0.00	0.00	0.00	0.00	0.00	0.00
Pf	0.00	0.00	0.00	0.00	0.00	0.00	0.00	0.00	0.00
Ap	1.49	1.53	1.46	1.59	1.50	1.05	1.00	1.36	1.65
Sum	98.91	98.98	99.52	99.44	99.01	99.40	99.48	98.93	99.37
DI	44.96	52.37	43.06	47.85	44.17	62.34	68.40	46.70	48.39
Ti (in ppm)	16,717.00	17,845.00	16,023.00	17,930.00	15,625.00	12,820.00	10,993.00	16,885.00	17,901.00
Rb	34.73	32.92	36.54	40.01	37.44	59.00	65.15	35.98	32.60
Cs	0.36	0.33	0.35	0.39	0.38	0.41	0.50	0.36	0.36
Sr	845.30	832.80	768.60	829.30	824.40	543.20	522.40	1030.80	792.60
Ba	603.90	643.30	572.70	599.10	642.30	408.20	430.70	617.70	588.80
Sc	24.90	23.60	22.80	23.90	21.00	16.80	15.30	22.80	26.50
V	241.70	226.50	220.90	239.90	214.00	169.50	141.00	227.00	251.60
Cr	289.00	246.00	350.00	283.00	337.00	156.00	125.00	273.00	402.00
Co	56.07	48.88	65.67	55.17	61.74	36.57	30.92	56.94	54.10
Ni	226.60	119.40	352.20	198.40	331.30	99.50	86.10	227.60	195.40
Zn	105.00	105.00	103.00	105.00	109.00	115.00	115.00	124.00	102.00
Zr	254.00	244.00	227.00	238.00	256.00	366.00	413.00	259.00	249.00
Nb	77.03	75.07	75.81	80.73	82.58	77.77	75.49	85.09	76.52
Hf	5.58	5.60	4.89	5.21	5.42	8.31	9.76	5.46	5.47
Ta	4.47	4.43	4.42	4.70	4.82	4.48	4.62	4.84	4.48
Pb	2.20	2.60	2.90	2.60	2.20	5.10	5.40	2.30	2.00
Th	5.16	5.70	5.13	5.44	5.61	7.63	8.85	5.53	5.13
U	1.34	1.34	1.35	1.38	1.43	1.66	1.76	1.36	1.35
Y	26.73	26.29	23.88	25.95	24.74	36.25	41.37	26.69	27.65
La	52.75	52.07	50.44	52.72	55.54	66.39	71.64	59.97	51.34
Ce	101.43	99.46	97.29	99.91	103.07	128.06	138.43	111.29	97.77
Pr	11.76	11.75	11.17	11.81	11.87	14.88	16.43	12.68	11.66
Nd	46.47	47.07	42.99	46.83	45.72	57.47	63.31	49.69	46.45
Sm	8.75	8.80	7.94	8.73	8.37	10.74	11.87	8.86	8.91
Eu	2.99	3.09	2.75	2.96	2.94	2.19	2.42	3.02	2.96
Gd	7.70	7.67	7.01	7.56	7.22	9.34	10.54	7.51	7.83

Table 3 continued

Samples	MV38 Noun Plain	FM40	FM41	FM42	FM43	ML44	ML45	MB46	MB47
Lithology	B(TB)	B(TB)	B(TB)	B(TB)	TB-H	BTA-M	TA-B	B(TB)	B(TB)
Tb	1.04	1.06	0.93	1.01	0.97	1.31	1.51	1.02	1.07
Dy	5.73	5.61	4.94	5.58	5.25	7.35	8.49	5.59	5.88
Ho	0.98	1.00	0.87	0.95	0.91	1.34	1.56	0.98	1.01
Er	2.56	2.53	2.21	2.42	2.38	3.60	4.25	2.55	2.63
Tm	0.33	0.32	0.29	0.31	0.30	0.49	0.57	0.32	0.33
Yb	1.95	1.91	1.69	1.85	1.78	3.03	3.56	1.98	2.00
Lu	0.27	0.28	0.25	0.25	0.25	0.44	0.52	0.27	0.28
La/Yb	27.08	27.29	29.93	28.56	31.29	21.93	20.15	30.23	25.71
Zr/Nb	3.30	3.25	2.99	2.95	3.10	4.71	5.47	3.04	3.25
Nb/U	57.45	55.94	56.03	58.50	57.63	46.74	42.89	62.56	56.76
La/Nb	0.68	0.69	0.67	0.65	0.67	0.85	0.95	0.70	0.67
Ba/Nb	7.84	8.57	7.55	7.42	7.78	5.25	5.71	7.26	7.70
(La/Yb)N	18.11	18.25	20.02	19.10	20.92	14.66	13.48	20.21	17.19
Th/Yb	2.65	2.99	3.05	2.95	3.16	2.52	2.49	2.79	2.57
Nb/Yb	39.55	39.35	44.99	43.73	46.52	25.68	21.24	42.89	38.32

BA Basaltic andesite, *AB* Alkaline basalt, *SAB* Sub-alkaline basalt, *TB-H* Trachy- basalt, *B* Basanite, *T* Tephrite, *BTA* Basaltic Trachy-andesite, *TA* Trachy-andesite

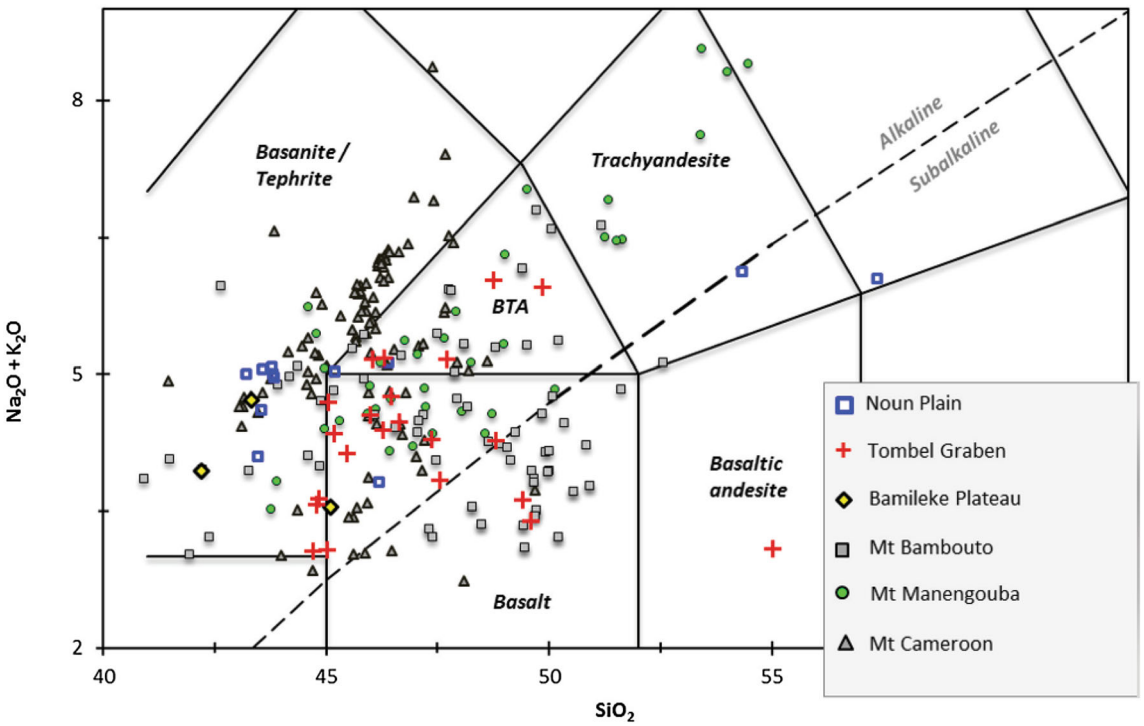

Fig. 6 Total alkali versus silica (TAS) classification diagram (Le Bas et al. 1986) for the analyzed pozzolans compared to lavas of the nearby large volcanoes

4.2 Mineralogy

Table 2 and Fig. 5 present the percentages of minerals and amorphous phases of the analyzed samples. For commodity, the names of minerals have been abbreviated in the text, according to Kretz (1983) to show the mineral assemblage in samples. In almost all samples, plagioclase and augite are the most dominant mineral phases, followed by olivine and Fe–Ti oxides. K-feldspar and nepheline are scarce. Samples from Barombi Kotto Island, Mt Koupe, Penja, and Manjo in the Tombel Plain contain primarily labradorite (26–56 wt%), augite (10–54 wt%), olivine (5–15 wt%), ilmenite (0.5–8 wt%), magnesite (0.7 wt% in only one sample), smectite (42.3 wt% in one sample), franklinite 7.1 wt% (in only one sample), Ti-magnetite, muscovite, hematite, nepheline, and calcite. The mineralogical assemblage comprises Lab + Aug + Ol + Ti-Mag + Mag ± Qtz ± Musc ± Ne ± K-Fpr ± Hem ± Cal ± Mags ± Ilm ± Gib ± Gt ± Fkl. In the Bamileke Plateau, the mineralogical assemblage is Aug + Lab + Ol ± Hem ± Mag ± Musc ± Ne ± Ti-Mag ± Gt, with augite ranging between 38 and 40 wt%, labradorite between 20 and 25 wt% and olivine between 5 and 7 wt%. Ti-magnetite, nepheline, hematite, and goethite are accessories. In the Noun Plain, the mineralogical assemblage is composed of Aug + Lab + Ol + Mag ± Qtz ± Musc ± Hem ± Cal ± Ne ± Ti-Mag ± Ilm ± Fkl ± Fl-Ap ± Hem. Samples exhibit augite (12–46%), labradorite (9–21%), olivine (5–27%) as main phases, while Ti-magnetite (1–3 wt%), quartz (< 1%) nepheline, hematite, franklinite, fluorapatite, hematite, and ilmenite as scare phases. The amorphous phase contents vary between 0 and 50.8 wt% in the Tombel Plain (average of 15.4 wt%), between 5.2 and 81.2 wt% in the Bamileke Plateau (average of 36.6 wt%) and, between 1.0 and 69.1 wt% in the Noun Plain (average of 31.7 wt%).

4.3 Major elements geochemistry

Major element compositions and calculated CIPW norm of the studied pozzolans are presented in Table 3. The SiO_2 content ranges from 42.20 to 45.10 wt% in the Bamileke Plateau, between 44.71–55.02 and 43.21–57.38 wt% in the Tombel and the Noun Plains, respectively. The Al_2O_3 content is quite constant (14.45–15.09 wt%) in the Bamileke Plateau in respect to the Tombel and Noun Plains where it varies between 12.08–19.44 and 11.99–15.83 wt%, respectively. The T-Fe_2O_3 content is also constant (13.39–14.66 wt%) in the Bamileke Plateau compared to the Tombel and Noun Plains where it ranges between 10.85–14.25 and 9.56–14.00 wt%, respectively. The CaO content varies between 9.59 and 11.03 wt% in the Bamileke

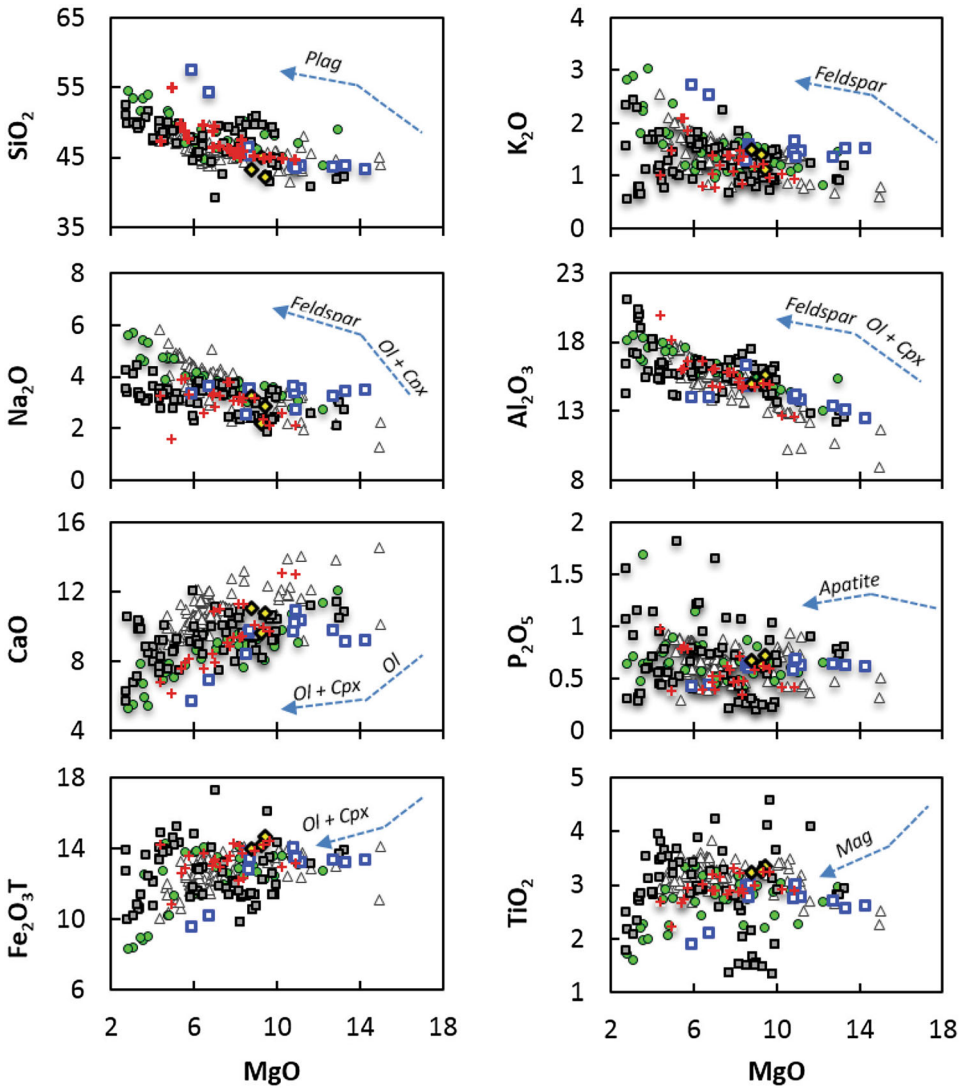

Fig. 7 The Tombel Plain, Bamileke Plateau and Noun Plain bivariate diagrams of major elements versus MgO for analyzed pozzolans compared to the CVL nearby volcanoes. Markers are as in Fig. 5

Plateau, between 6.16–13.06 and 5.56–10.87 wt% in the Tombel and Noun Plains, respectively. Lavas from Noun Plain are the most magnesium-rich types with MgO varying between 5.40 and 13.77 wt% compared to those in Bamileke Plateau and Tombel Plain between that display 8.29–8.96 wt% 3.61–10.38 wt% respectively. The total alkali ($Na_2O + K_2O$) varies between 3.55 and 4.72 wt% in the Bamileke Plateau, from 3.06 to 6.03 wt% in the Tombel and 3.81–6.12 wt% in the Noun Plains. Most of the samples present acceptable LOI values $\leq$ 4 wt% (Table 1). However, a few of them (BKI 48, TL09, TPja13, BL32, and N34) present values between 4 and 8.51 wt%. These might be considered as weathered (Crummy et al. 2014) and will be used with caution in further petrological interpretations.

The CIPW norm reveals normative nepheline and olivine on half of the studied sample. The Tombel Plain pozzolans display lowest values of normative nepheline (0–5.8 wt%) and olivine (0–10.40 wt%) while those from Bamileke Plateau and Noun Plain exhibit high- to highest-value of normative nepheline (4.30–24.92 wt%) and olivine (10.53–21.39 wt%) apart the tephritic sample BL31 with Ol = 8.26 wt%.

Figure 6 highlights the variability of rock types. Amongst the 24 samples studied in the Tombel Plain, there are 13 alkaline basalts, five sub-alkaline basalts, five trachybasalts, and one basaltic andesite. The Noun Plain includes seven tephrites and basanites, two trachybasalts, one alkaline basalt, one basaltic trachyandesite, and one trachy-andesite. The Bamileke Plateau samples are two basanites and one alkaline basalt.

Figure 7 shows bivariate plots of selected major elements (SiO_2, TiO_2, CaO, K_2O, Al_2O_3, FeO, and Fe_2O_3) versus MgO. The analyzed lavas along with lavas from neighborhood Mt Cameroon, Mt Manengouba, and Mt Bambouto volcanoes define continuous trends in most of these variation diagrams with a decrease in SiO_2, Al_2O_3,

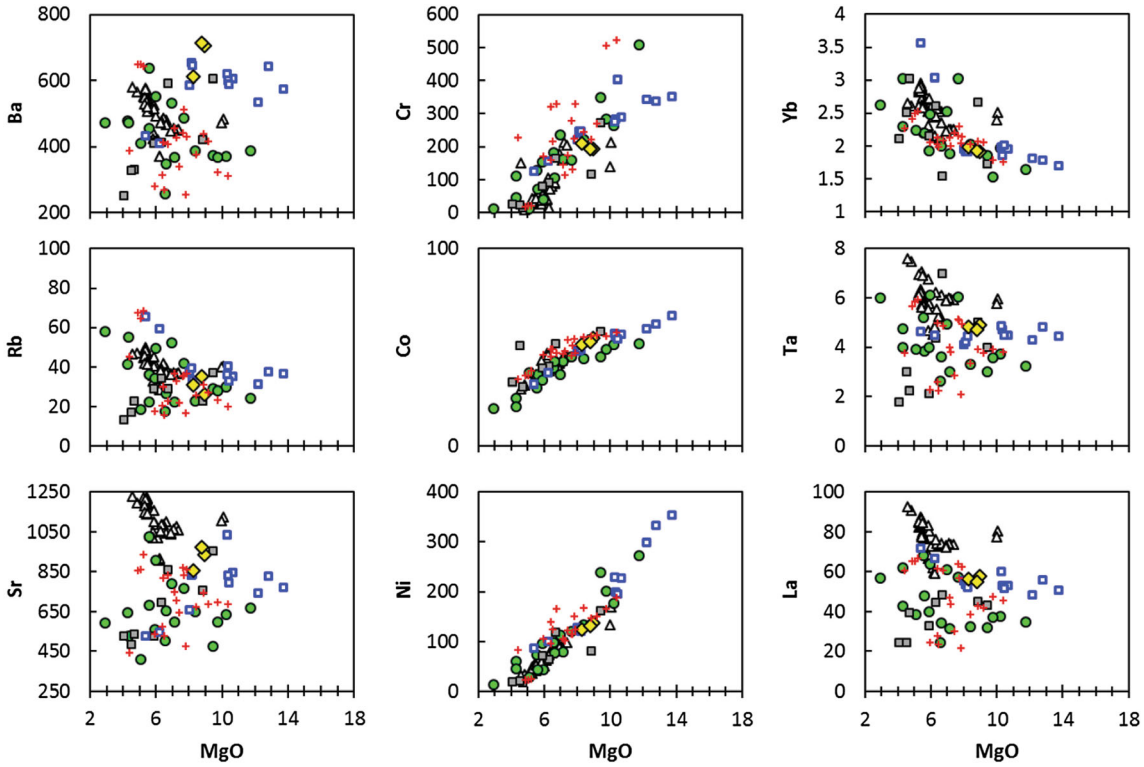

Fig. 8 The Tombel Plain, Bamileke Plateau, and Noun Plain trace elements variations versus MgO for analyzed pozzolans compared to the CVL nearby volcanoes. Markers are as in Fig. 5

and Fe_2O_3 as MgO increases. Contrarily, the FeO, K_2O, Na_2O, CaO, and TiO_2 generally increase as MgO increases.

4.4 Trace elements composition

Table 3 reports the trace elements (ppm) compositions of the studied samples and Fig. 8 shows bivariate plots of selected high field strength elements (HFSE), large-ions lithophile elements (LILE) and transition elements against MgO. HFSE's display a slight negative correlation with MgO in the Tombel Plain. Apart from Hf and Y (not shown) that follow the same trend as in Tombel Plain, HFSE's remain constant in the Bamileke plateau and Noun Plain (Fig. 8). LILE such as Rb, Cs, and Sr, are also constant with increasing MgO in the Noun plain. Samples of the Tombel Plain can be discriminated between enriched- and poor-LILE; the enriched-LILE lava patterns decrease as MgO increases until ~ 8 wt% while the poor-LILE lavas patterns increase as MgO rises until ~ 8 wt% (Fig. 8). The transition elements (Ni, Cr, Co) exhibit a positive correlation with increasing MgO for all samples irrespective of the volcanic field. Scandium and V (plots not shown) follow the same trend for all the samples from Tombel plain but remain constant for samples from Bamileke plateau and Noun plain.

Figure 8 shows the studied lavas normalized to primitive mantle multi-elements patterns compared with nearby large stratovolcano samples. The Tombel Plain samples are compared with those of Mt Cameroon and Mt. Manengouba (Fig. 9a), while Noun Plain and Bamileke Plateau samples are compared with those of Mt Bambouto (Fig. 9b). All samples follow the same pattern with their nearby volcanoes and show a general OIB-like pattern (Fig. 9a, b). An enrichment of LREE relative to HREE is evident with negative anomalies in some compatible elements such as Cs, Rb, U, Th, and Pb, and a positive anomaly in one incompatible element (Nb).

5 Discussions

5.1 Crystal fractionation

The overall mafic composition ($SiO_2 < 52$ wt%) of the studied samples (Fig. 5) with high MgO values (up to 10.38 wt% in Tombel plain, ~ 8 wt% in Bamileke Plateau and between 8.04 and 13.77 wt% in Noun Plain) and Cr, Ni, and Co contents, which overlap with the expected composition for melts equivalents to primitive magma (Cr; 300–500 ppm, Ni; 300–400 ppm, Co; 50–70 ppm Beier et al. 2006, 2008; Madureira et al. 2011) suggest rapid

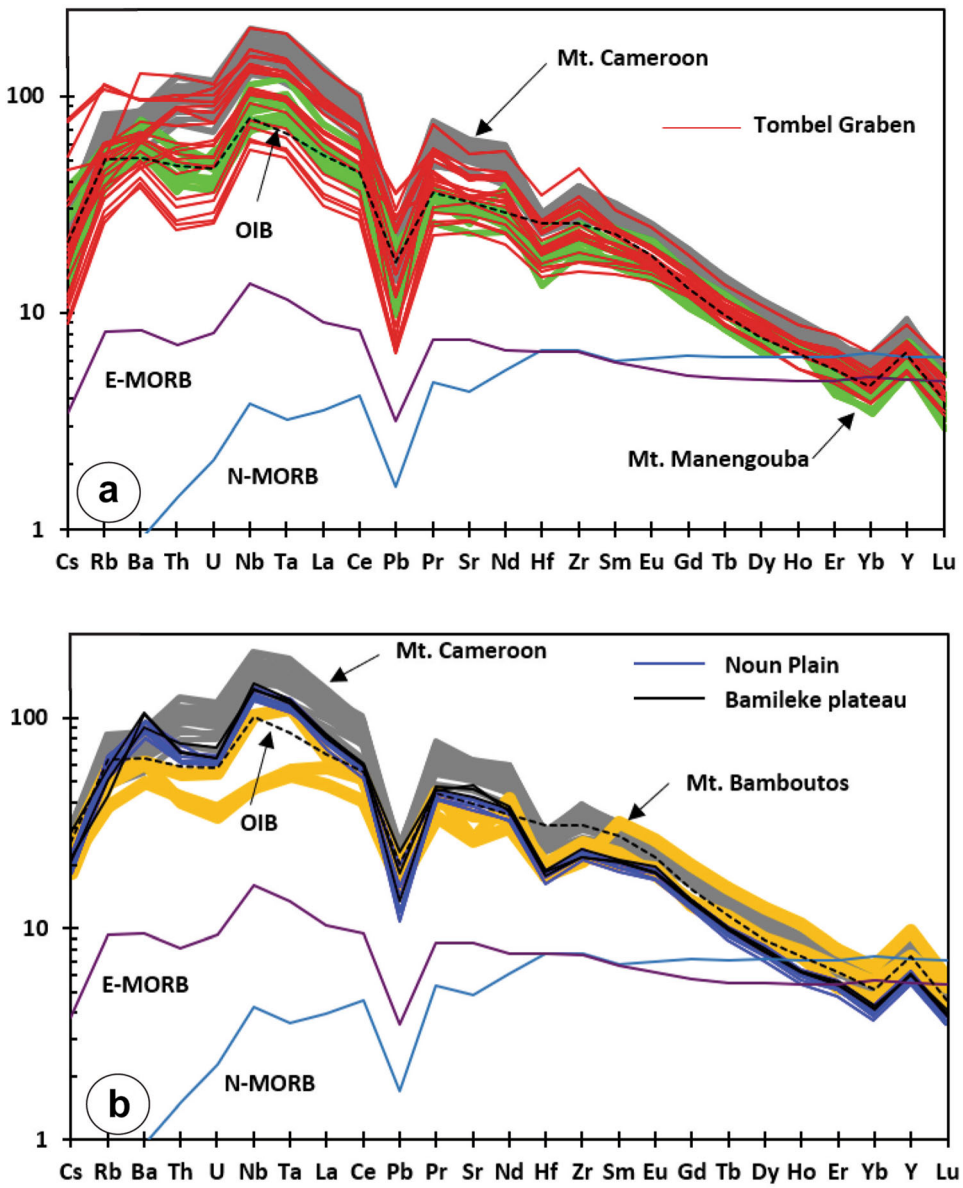

Fig. 9 Primitive-mantle-normalized (Sun and McDonough 1989) multi-element diagrams for **a** the Tombel Plain, **b** Bamileke Plateau and Noun Plain analyzed pozzolans from compared to the CVL nearby volcanoes

magma ascend. Consequently, a significant effect of the crystallization process during their ascension to the surface cannot be expected. This could be supported by the significant contents in amorphous phase in most samples (Table 1) even though the positive trends of transitions elements such as Co, Cr, Ni (Fig. 8) against MgO (Brenna et al. 2010) and the negative trends of Al_2O_3 and Na_2O (Fig. 7) against MgO highlight fractionation of both olivine and clinopyroxene minerals. The mafic character and overall nearly primitive melt composition indicate that these samples can be used to discuss the nature and source composition of their magmas though it is primarily essential to check if those magmas did not suffer crustal assimilation during their passing through the Earth crust.

5.2 Crustal contamination

Crustal contamination has already been evidenced in many CVL igneous rocks (e.g., Marzoli et al. 1999; Rankenburg et al. 2005; Kamgang et al. 2008, 2013; Tchuimegnie Ngongang et al. 2015). The assimilation of crustal melts by a rising magma can increase its contents in some incompatible elements. Hart et al. (1989) indicated for example, that rising magmas that have faced crustal assimilation on passing through the thick continental crust could have ratios of La/Nb > 1.5 and La/Ta > 22. Such magmas also are expected to have a composition (Nb/Yb and Th/Yb ratios) that deviates from that of mid-ocean ridge basalts (MORB) or OIBs (Pearce 2008; Pearce et al. 1995). Our studied samples present La/Nb ratios between 0.6 and 0.9

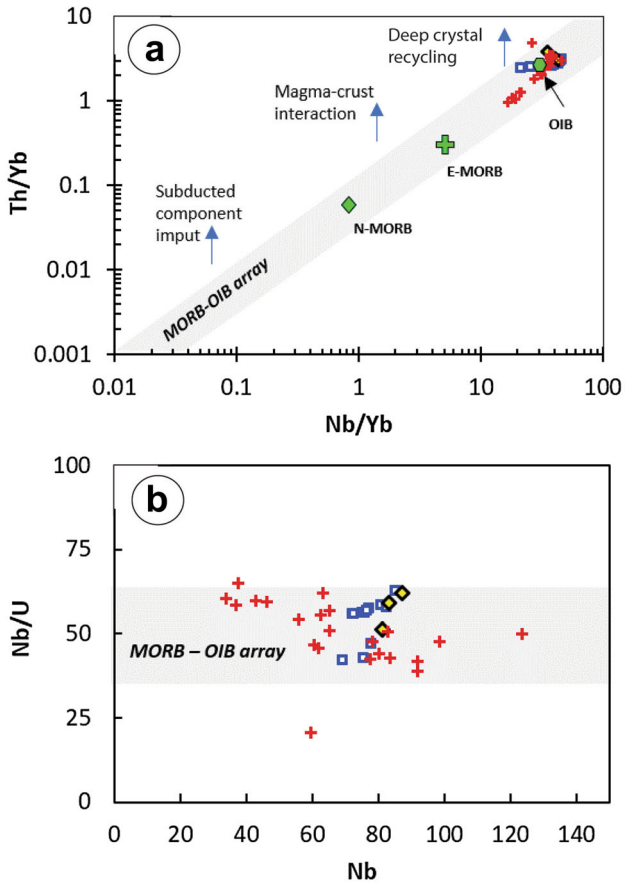

Fig. 10 Diagrams of Th/Yb versus Nb/Yb and Nb/U versus Nb showing the OIB signature of the pozzolans (after Pearce and Peate 1995; Pearce 2008). N-MORB, E-MORB, and OIB data from (Sun and McDonough 1989). Markers are as in Fig. 5

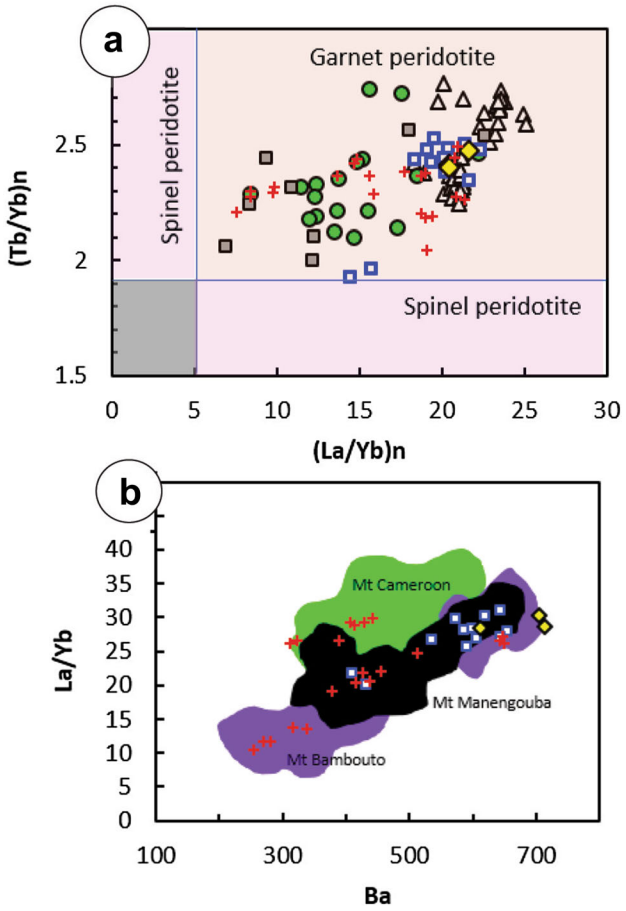

Fig. 11 Mantle sources and CVL relationships of the Tombel Plain, Bamileke Plateau, and Noun Plain pozzolans. **a** The plot of chondrite-normalized ratios of Tb/Yb and La/Yb to distinguish between spinel and garnet mantles. Chondrite values from Sun and McDonough (1989). Horizontal line, according to Wang et al. (2002). **b** Fields defined for samples from Mt Cameroon, Mt Bambouto and Mt Manengouba. Note the distribution of our samples in the different fields especially samples from the Tombel Plain with similarities with those from Mt Cameroon, Mt Bambouto and Mt Manengouba. Markers are as in Fig. 5

and La/Ta between 10.4 and 16.04. They also plot within the MORB-OIB array in the Nb versus Nb/U and Nb/Yb versus Th/Yb (Fig. 10) that suggests a negligible contribution of crustal materials. This aligns with their high-MgO values, the lack of a negative Nb–Ta spike on the primitive mantle-normalized multi-elements and the ratios of some other incompatible elements such as Zr/Nb (3–5), and Ba/Nb (6.1–8.5) that equal those of OIBs (Weaver 1991; Sun and McDonough 1989).

5.3 Mantle sources

The studied samples, as demonstrated above, exhibit an OIB affinity like most volcanic lavas of the CVL (Asaah et al. 2015; Kamgang et al. 2013; Ngwa et al. 2017; Suh et al. 2009; Yamgouot et al. 2016). They also show a composition that overlaps those of nearby volcanoes, suggesting that their magmas were certainly generated in similar sources in the mantle. Most of the CVL magmas derive from the melting of mantle rocks, dominantly within the garnet lherzolite stability field (Asaah et al. 2015; Atouba et al. 2016) although cases of melting in the mantle spinel lherzolite field (Lee et al. 1994; Nkouandou and Temdjim 2011) and the participation of pyroxenites have been reported (Kamgang et al. 2008; Tchuimegnie Ngongang et al. 2015). Using the ratios of La and Yb normalized to chondrite values, $(La/Yb)_N$, Farmer (2003) suggested that lavas with a $(La/Yb)_N \leq 5$ and those with a $(La/Yb)_N \geq 5$ derived from melting in spinel and a garnet lherzolite stability zone respectively. Accordingly, the highest $(La/Yb)_N$ i.e. 7–20 of our lavas suggests that their parental magmas originated from partial melting in a dominantly garnet-bearing mantle zone (Fig. 11a), i.e., at depths greater than 80 km. This can be supported by their $(Tb/Yb)_N > 1.9$ (Wang et al. 2002). Still, the variations in trace elements compositions (La/Yb, Ba) of the studied

samples might indicate either heterogeneity in the mantle source or variations in the degree of partial melting as shown by samples from the Tombel Plain that share features of both Mt Cameroon, Mt Manengouba, and Mt Bambouto magmas (Fig. 11b).

5.4 Pozzolanicity hints: influence of the mineralogy to the suitability of studied pozzolans in cement manufacturing

Portland cement remains the best cement used in the industry nowadays. However, because of its high cost and that of its main constituent, the clinker, the use of pozzolans compliant with standards such as NF EN 197-1 and ASTM C-618 remains a good alternative. The abundance and accessibility of pozzolans in the southern and central continental portions of the CVL might thus represent a prime material for the local industries. However, a pozzolan should present a certain quality, especially an excellent activity to be used as an additive in cement manufacturing and depends directly on its chemical and mineralogical compositions (Walker and Pavía 2011). The mineralogy and reactivity relationships of aggregates mainly obey to amorphous silica or cryptocrystalline content (Lombardi et al. 1997; Prezzi et al. 1997, 1998). Also, the abundance of amorphous phases in a pozzolan is demonstrated to increase its reactivity or pozzolanicity (Pichon 1994; Segui 2011) improving, therefore, the mechanical properties of the pozzolan by promoting the cohesion and densification by the elimination of porosity (Weshondo 2012).

Though determining the pozzolanicity of our samples was out of the scope of the present paper, the extensive usage of these deposits in the cement factory might also be related to their mineralogical composition. For instance, most of our studied samples display a significant (> 10 %) amorphous phases content (Table 2, Fig. 5a), up to 50 % for Kpé04, Kpé07, and TL08 in the Tombel plain (Fig. 5b); to 81.2 % for BL32 in the Bamileke Plateau (Fig. 5c); and to 69.1 for MV38 in the Noun Plain (Fig. 5d); suggesting that they could present an interesting pozzolanicity, and therefore usable as additive in cement factory. The pozzolanicity of a natural pozzolan can also be appreciated based on the sum of SiO_2, Al_2O_3, and Fe_2O_3T (SAI) or their sum of CaO, FeO and MgO (CIM) since those oxides allow the development of vitreous phase whereas other oxides such as Na_2O are against amorphous phase formation (Weshondo 2012). According to the ASTM C 618 standard, a good pozzolan must have an SAI greater than 70 wt%. The SAI of our studied pozzolans vary from 68.50 to 83.50 wt% indicating that they almost all would fulfill the requirement of the standard. However, their CIM vary widely, between 14.5 and 30.52 wt% in the Tombel plain, between 20.67 to 22.03 wt% in the Bamileke plateau, and between 23.58 and 31.08 wt% in the Noun Plain. Two sets of samples can thus be distinguished; the first one with CIM far less than 29% and the second one made up of samples having a sum CIM > 29 %. The latter set of pozzolans with CIM > 29 wt% could be considered the more prone to develop an amorphous phase that governs the reactivity of pozzolans. From that point of view, only two pozzolans from Tombel plain (Lim53 and Lim54) and four from Noun Plain (ML37, MV38, FM43, and MB46) that present a relatively high amount of CIM (> 29 wt%) seem to be suitable as an additive in cement manufacture. A detailed study is being carried out in order to verify this hypothesis.

6 Conclusion

The mineralogical and geochemical studies of pozzolan deposits from Tombel Plain, Bamileke Plateau, and Noun Plain in the continental portion of the CVL have been realized to assess their petrology and their possible pozzolanicity or ability to be used as additives for cement manufacture. In summary, the studied samples comprise alkaline and subalkaline basalts, trachy-basalts, and basanites. They exhibit an OIB affinity, and alike most volcanic lavas of the CVL, their composition suggests that their magmas were generated in a dominantly garnet-bearing mantle zone. Though the insignificant effect of crustal contamination and crystal fractionation were noticed, the variations in trace element compositions (La/Yb, Ba) suggest either heterogeneity in the mantle source or variations in the degree of partial melting. The main mineralogical assemblages including augite, plagioclase, followed by Fe–Ti oxides and olivine, with few K-feldspar, nepheline, and quartz as accessory phases, as well as high glass content of most samples, suggest their occurrence through the rapid ascent of the magma. According to their Activity Index (AI), the studied pozzolans, especially those in the Tombel Graben, with important amorphous phases, seem to be suitable as additives for cement manufacture. Additional tests providing information on Compressive Strength, SAI and durability that form part of ASTM C 618 requirements are being carried out to confirm the real importance of those materials in cement manufacture.

Acknowledgements Authors are thankful to the ISTerre of Grenoble (France) and Nathaniel Findling for hosting and training the first author on the XRD technique and Rietveld method interpretation as part of his Ph.D. research work. The authors are also thankful to the Ministry of Higher Education of Cameroon for providing Research Modernization Allowance (RMA) that has been very helpful to support part of the field trip and Geochemical analysis expenses.

References

Aka FT, Ngako K, Kusakabe M, Sumino H, Tanyileke G, Ateba B, Hell J (2004) Symmetrical helium isotope distribution on the Cameroon volcanic line, West Africa. Chem Geol 203:205–223

Aka FT, Yokohama T, Kusakabe M, Nakamura E, Tanyileke G, Ateba B, Ngako V, Nnange JM, Hell JV (2008) U-series dating of Lake Nyos maar basalts, Cameroon (West Africa); implications for potential hazards on the Lake Nyos dam. J Volcanol Geotherm Res 176:212–224

Asaah ANE, Yokoyama T, Aka FT, Usui T, Wirmvem MJ, Chako Tchamabe B, Ohba T, Tanyileke G, Hell JV (2015) A comparative review of petrogenetic processes beneath the Cameroon Volcanic Line: geochemical constraints. Geosci Front. https://doi.org/10.1016/j.gsf.2014.04.012

Asaah ANE, Yokoyama T, Aka FT, Iwamori H, Kuritani T, Usui T, Gountie Dedzo M, Tamen J, Hasegawa T, Fozing EM, Wirmvem MJ, Nche AL (2020) Major/trace elements and Sr–Nd–Pb isotope systematics of lavas from lakes Barombi Mbo and Barombi Koto in the Kumba graben. Cameroon Volcan Line Constr Petrog J Afr Earth Sci. https://doi.org/10.1016/j.jafrearsci.2019.103675

ASTM C 618-15, Standard Specifications for Coal Fly Ash and Raw or Calcined Natural Pozzolan for Use in Concrete. ASTM International, West Conshohocken, PA, 2015

Atouba LCO, Chazot G, Moundi A, Agranier A, Bellon H, Nonnotte P, Nzenti JP, Kankeu B (2016) Mantle sources beneath the Cameroon Volcanic Line: geochemistry and geochronology of the Bamoun plateau mafic rocks. Arab J Geosci. https://doi.org/10.1007/s12517-015-2285-6

Ballentine CJ, Lee DC, Halliday AN (1997) Hafnium isotopic studies of the Cameroon line and new HIMU paradoxes. Chem Geol 139:111–124

Bardintzeff JM, McBirney AR (2000) Volcanology. Jones and Bartlett, Sudbury, p 288

Beier C, Haase KKM, Hansteen TH (2006) Magma evolution of the Sete Citades Volcano, São Miguel, Azores. J Petrol 47:1375–1411

Beier C, Haase KKM, Abouchami W, Krienitz MS, Hauff F (2008) Magma genesis by rifting of oceanic lithosphere above anomalous mantle: Terceira Rift, Azores. Geochem Geophys Geosyst 9:Q12013

Billong N, Melo U, Njopwouo D, Louvet F, Bonnet J (2013) Physicochemical characteristics of some Cameroonian pozzolans for use in cement-like materials. Mat Sci Appl 1:14–21

Brenna M, Cronin SJ, Smith IEM, Sohn YK, Ne´meth K (2010) Mechanism driving polymagmatic activity at a monogenetic volcano, Udo, Jeju Island, South Korea. Contrib Miner Petrol 160:931–950

Cantagrel J-M, Jamoud C, Lasserre M (1978) Le magmatisme alcalin de la Ligne du Cameroun au Tertiaire inférieur: données géochronologiques K-Ar. CR Soc Géol Fr 6:300–310

Chako Tchamabe B (2014) Volcano-stratigraphy and geochemistry of tephra deposits and its relevance for understanding the polygenetic inheritance and plumbing systems to maar-diatreme volcanoes: clues for hazards perspective, a case study for the Barombi Mbo Maar, Cameroon, central Africa. Dissertation, Tokai University, Japan

Crummy JM, Savoy IP, Navarro-Ochoa C, Morgan DJ, Wilson M (2014) High-K Mafic Plinian Eruptions of Volcán de Colima Mexico. J Petrol 55:2155–2192

Déruelle B, Ngounouno I, Demaiffe D (2007) The "Cameroon Hot Line" (CHL): a unique example of active alkaline intraplate structure in both oceanic and continental lithospheres. C R Geosci 339(9):589–600

Doebelin N, Kleeberg R (2015) Profex: a graphical user interface for the Rietveld refinement program BGMN. J Appl Cryst 48:1573–1580

Erlund EJ, Cashman KV, Wallace PJ, Pioli L, Rosi M, Johnson E, Delgado Granados H (2010) Compositional evolution of magma from Paricutin Volcano, Mexico: the tephra record. J Volcanol Geotherm Res 1–4:167–187

Farmer GL (2003) Continental basaltic rocks. In: Treatise on geochemistry, Vol 3. Editor: Roberta L Rudnick executive editors: Heinrich D Holland, Karl K Turekian. 659 p. Elsevier, 85–121, ISBN 0-08-043751-6

Fitton JG, Dunlop HM (1985) The Cameroon Line, West Africa, and it's bearing on the origin of oceanic and continental alkali basalts. Earth Planet Sci Lett 72:23–38

Geoscience Laboratories (2015) Schedule of fees and services. Geolab, Effective April 1, 2015, 7

Halliday AN, Dickin AP, Fallick AE, Fitton JG (1988) Mantle dynamics: a Nd, Sr, Pb, and isotopic study of the Cameroon Line Volcanic chain. J Petrol 29:181–211

Halliday AN, Davidson JP, Holden P, Dewolf C, Lee DC, Fitton JG (1990) Trace—element fractionation in plumes and the origin of HIMU mantle beneath the Cameroon Line. Nature 347(6293):523–528

Hart WK, Wolde GC, Walter RC, Mertzman SA (1989) Basaltic volcanism in Ethiopia: constraints on continental rifting and mantle interactions. J Geophys Res 94:7731–7748

Hasegawa T, Aka FT, Miyabuchi Y, Anye Nche L, Kobayashi T, Kaneko K, Asaah ANE, Kankeu B, Ohba T, Kusakabe M, Hell JV (2019) Eruption history and petrogenesis of rocks from Nyos volcano (NW Cameroon): evidence from lithostratigraphy and geochemistry. J Volcanol Geoth Res 378:51–71

Hillier S (2003) Quantitative analysis of clay and other minerals in sandstones by X-ray powder diffraction (XRPD). In: Worden RH, Morad S (eds) Clay mineral cements in sandstones: international association of sedimentologists, vol 34. International Association of Sedimentologists. Sp Publ, Prague, pp 213–251

Janousek V, Farrow CM, Erban V (2006) Interpretation of whole-rock geochemical data in igneous geochemistry: introducing Geochemical Data Toolkit (GCDkit). J Petrol 47(6):1255–1259

Jenkins R, Snyder RL (1996) Introduction to X-ray powder diffractometry. Wiley, Hoboken

Kamgang P, Chazot G, Njonfang E, Tchoua F (2008) Geochemistry and geochronology of mafic rocks from Bamenda Mountains (Cameroon): source composition and crustal contamination along the Cameroon Volcanic Line. C R Geosci 340(12):850–857

Kamgang P, Chazot G, Njonfang E, Tchuimegnie NNB, Tchoua FM (2013) Mantle sources and mantle evolution beneath the Cameroon Volcanic Line: geochemistry of mafic rocks from Bamenda Mountains (NW Cameroon). Gondwana Res 24:727–741

Kereszturi G, Nemeth K, Csillag G, Balogh K, Kova'cs J (2011) The role of external environmental factors in changing eruption styles of monogenetic volcanoes in a Mio/Pleistocene continental volcanic field in western Hungary. J Volcanol Geotherm Res 201(1–4):227–240

Kretz R (1983) Symbols of rock-forming minerals. Am Miner 68:277–279

Le Bas MJ, Le Maître RW, Streckeisen A, Zanettin B (1986) A chemical classification of volcanic rocks based on the total alkali-silica diagram. J Petrol 27:745–750

Lee DC, Halliday AN, Fitton JG, Poli G (1994) Isotopic variations with distance and time in the volcanic island of the Cameroon Line— evidence for a mantle plume origin. Earth Planet Sci Lett 123:119–138

Lombardi J, Massard P, Perruchot A (1997) Mesure expérimentale de la cinétique de formation d'un gel silicocalcique, produit de la réaction alcalis-silice. Cemt Concr Res 27(9):1379–1391

Madsen IC, Scarlett NVY, Kern A (2011) Description and survey of methodologies for the determination of amorphous content via X-ray powder diffraction. Z Krist 226:944–955

Madureira P, Mata J, Mattielli N, Quiroz G, Silva P (2011) Cement and concrete research: constraints from elemental and isotopic (Sr, Nd, Hf, Pb) data. Lithos 126:402–418

Martin U, Nemeth K (2006) How Strombolian is a ''Strombolian'' scoria cone? Some irregularities in scoria cone architecture from the Trans-Mexican Volcanic Belt, near Volcan Ceboruco, (Mexico) and Al Haruj (Libya). J Volcanol Geotherm Res 155(1–2):104–118

Marzoli A, Renne PR, Piccirillo EM, Castorina F, Bellieni G, Melfi AR, Nyobe JB, N'ni J (1999) Silicic magmas from the continental Cameroon Volcanic Line (Oku, Bambouto and Ngaoundere): ^{40}Ar–^{39}Ar dates petrology, Sr–Nd–O isotopes and their petrogenetic significances. Contrib Mineral Petrol 135:133–150

Massazza F (2007) Pozzolana and pozzolanic cements. In: Hewlett PC (ed) Lea's chemistry of cement and concrete, 4th edn. Elsevier, Kidlington, pp 47–602

McGee LE, Smith IEM (2016) Interpreting chemical compositions of small-scale basaltic systems: a review. J Volcanol Geotherm Res 325:45–60

McGee LE, Millet M-A, Smith IEM, Nemeth K, Lindsay JM (2012) The inception and progression of melting in a monogenetic eruption: Motukorea volcano, the Auckland volcanic field, New Zealand. Lithos 155:360–374

McGee LE, Smith IEM, Millet M-A, Handley HK, Lindsay JM (2013) Asthenospheric control of melting processes in a monogenetic basaltic system: a case study of the Auckland Volcanic Field. New Zealand. J Petrol 54(10):2125–2153

Morrissey M, Zimanowski B, Wohletz K, Bütnner R (2000) Phreatomagmatic fragmentation. In: Sigurdsson H (ed) Encyclopedia of Volcanoes. Academic Press, Cambridge, pp 431–445

Moundi A, Wandji P, Ghogomu Tanwi R, Bardintzeff J-M, Njilah KI, Foumboure I, Ntieche B (2009) Existence of quaternary ankaramites among Tertiary flood basalts at Koutaba (Bamoun Plateau, Western Cameroon): petrology and isotope data. Rev Bul Geol Soc 70(1–3):115–124

Nemeth K, Kereszturi G (2015) Monogenetic volcanism: personal views and discussion. Int J Earth Sci 104(8):2131–2146

Nemeth K, White JDL, Reay A, Martin U (2003) Compositional variation during monogenetic volcano growth and its implications for magma supply to continental volcanic fields. J Geol Soc Lond 160:523–530

NF EN 197 – 1; Caractéristiques des ciments courants et de leurs constituants. Partie 1: Composition, spécifications, et critères de conformité des ciments courants. AFNOR, Avril 2012

Ngwa CN, Hansteen TH, Devey C, van der Zwan W, Froukje M, Suh CE (2017) Origin and evolution of primitive melts from the Debunscha Maar, Cameroon: consequences for mantle source heterogeneity within the Cameroon Volcanic Line. Lithos 288:326–337

Nkouandou OF, Temdjim R (2011) Petrology of spinel lherzolite xenoliths and host basaltic lava from Ngao Voglar Volcano, Adamawa Massif (Cameroon Volcanic Line, West Africa): equilibrium conditions and mantle characteristics. J Geosci 56(4):375–387

Nkouathio DG (2006) Evolution tectono-magmatique et volcanologique de la Ligne du Cameroun: comparaison d'un volcanisme de graben (plaine de Tombel) et d'un volcanisme de horst (monts Bambouto). Dissertation, Université de Yaoundé I, Cameroun. p 231

Nkouathio DG, Kagou Dongmo A, Bardintzeff J-M, Wandji P, Bellon H, Pouclet A (2008) Evolution of volcanism in graben and horst structures along the Cenozoic Cameroon Line (Africa): implications for tectonic evolution and mantle source composition. Miner Petrol 94:287–303

Pearce JA (2008) Geochemical fingerprinting of oceanic basalts with applications to ophiolite classification and the search for Archean oceanic crust. Lithos 100:14–48

Pearce JA, Peate DW (1995) Tectonic implications of volcanic arc Magmas. Annu Rev Earth Planet Sci 23:251–285

Pearce JA, Baker PE, Harvey PK, Luff IW (1995) Geochemical evidence for subduction fluxes, mantle melting and fractional crystallization Beneath the South Sandwich Island Arc. J Petrol 36:1073–1109

Pichon H (1994) Le système « pouzzolanes naturelles-chaux-eau » à 38 et 100RC. Relations entre la réactivité chimique, les phases néoformées et les conséquences mécaniques (application aux matériaux volcaniques du Massif Central Français). Dissertation, Université de Grenoble, p 234

Prezzi M, Monteiro PJM, Sposito G (1997) The alkali–silica reaction, part I: use of the double layer theory to explain the behavior of reaction-product gels. ACI Mater J 94(1):10–17

Prezzi M, Monteiro PJM, Sposito G (1998) The alkali–silica reaction, Part II: the effect of chemical admixtures. ACI Mater J 95(1):3–10

Rankenburg K, Lassiter JC, Brey JP (2005) The role of continental crust and lithospheric mantle in the genesis of Cameroon Volcanic Line lavas: constraints from isotopic variations in lavas and megacrysts from the Biu and Jos Plateau. J Petrol 46(1):169–190

Raven MD, Self PG (2017) Outcomes of 12 years of the Reynolds cup quantitative mineral analysis round Robin. Clay Clay Miner 65:122–134

Rodriguez-Camacho RE, Uribe-Afif R (2002) Importance of using the natural pozzolans on concrete durability. Cem Concr Res 32:1851–1858

Sato H, Aramaki S, Kusakabe M, Hirabayashi J-I, Sano Y, Nojiri Y, Tchoua FM (1990) Geochemical difference of basalts between polygenetic and monogenetic volcanoes in the central part of the Cameroon volcanic line. J Geochem Soc Jpn 24:357–370

Segui P (2011) Elaboration de liants hydrauliques routiers à base de pouzzolane naturelle ou de cendre volante de papeterie. Dissertation, Toulouse III Paul Sabatier, p 210

Smith IEM, Blake S, Wilson CJN, Houghton BF (2008) Deep-seated fractionation during the rise of a small-volume basalt magma batch: crater Hill, Auckland, New Zealand. Contrib Miner Petrol 155(4):511–527

Suh CE, Stansfield SA, Sparks RSJ, Njome MS, Wantim MN, Ernst GGJ (2009) Morphology and structure of the 1999 lava flows at Mount Cameroon Volcano (West Africa) and their bearing on emplacement dynamics of volume-limited flows. Geol Mag 148:22–34

Sun SS, McDonough NF (1989) Chemical and isotopic systematics of oceanic basalts: implications for mantle composition and processes. Geol Soc Sp Pub 42:313–345

Tamen J, Nkoumbou C, Mouafo L, Reusser E, Tchoua FM (2007) Petrography and geochemistry of monogenetic volcanoes of the Barombi Koto volcanic field (Kumba graben, Cameroon Volcanic Line): implications for the mantle source characteristics. C R Géosci 339:799–809

Tchamdjou JWH, Moulay CT, Abidi L, Pereira-de-Oliveira Luiz A (2017) The use of volcanic scoria from 'Djoungo' (Cameroon) as cement replacement and fine aggregate by sand substitution in mortar for masonry. Eur J Environ Civ Eng. https://doi.org/10.1080/19648189.2017.1364298

Tchuimegnie Ngongang NB, Kamgang P, Chazot G, Agranier A, Bellon H, Nonnotte P (2015) Age, geochemical characteristics and petrogenesis of Cenozoic intraplate alkaline volcanic rocks in the Bafang region, West Cameroon. J Afr Earth Sci 102:218–232

Tiabou AF, Temdjim R, Ngwa NC, Che VB, Mebara OFX (2015) Polymagmatic processes at monogenetic volcanoes: insights from Baossi Monogenetic Lava Flows, Adamawa Plateau, Cameroon Volcanic Line. J Geogr Geol 7(2):56–69

Tiabou AF, Temdjim R, Wandji P, Bardintzeff J-M, Bih Che VB, Tibang BEE (2019) Baossi-Warack monogenetic volcanoes, Adamawa Plateau, Cameroon: petrography, mineralogy, and geochemistry. Acta Geochim 38(1):40–67

Van Otterloo J, Raveggi M, Cas RAF, Maas R (2014) Polymagmatic activity at the monogenetic Mt Gambier Volcanic Complex in the Newer Volcanics Province, SE Australia: new insights into the occurrence of intraplate volcanic activity in Australia. J Petrol 55(7):1317–1351

Valentine GA, Krier DJ, Perry FV, Heiken G (2007) Eruptive and geomorphic processes at the Lathrop Wells scoria cone volcano. J Volcanol Geotherm Res 161(1–2):57–80

Walker R, Pavía S (2011) Physical properties and reactivity of pozzolans, and their influence on the properties of lime-pozzolan pastes. Mater Struct 44:1139–1150

Wandji P, Bardintzeff J-M, Ménard J-J, Tchoua MF (2000) The alkaline fassaite-bearing volcanic province of the Noun Plain (West-Cameroon). Neues Jahrb Mineralogie-Monatshefte 1:1–14

Wang K, Plank T, Walker JD, Smith EI (2002) A mantle melting profile across the basin and range, SW USA. J Geophys Res 107:1–21

Weaver BL (1991) The origin of ocean island basalt end-member composition: trace element and isotopic constraints. Earth Planet Sci Lett 104:381–397

Weshondo OD (2012) Caractérisation et valorisation des matériaux argileux de la province de Kinshasa (RD Congo). Dissertation, Université de Liège, Belgique, p 337

Wotchoko P, Wandji P, Bardintzeff J-M, Bellon H (2005) Données pétrologiques et géochronologiques nouvelles sur le volcanisme alcalin néogène à récent de la rive ouest du Noun (plaine du Noun, Ligne du Cameroun). Rev Bulg Geol Soc 66:97–105

Yamgouot FN, Déruelle B, Mbowou IBG, Ngounouno I, Demaiffe D (2016) Geochemistry of the volcanic rocks from Bioko Island ("Cameroon Hot Line"): evidence for plume-lithosphere interaction. Geos Front 7(5):743–757

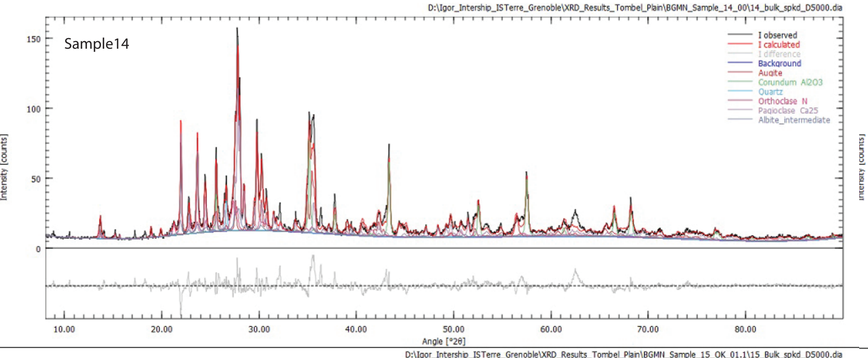

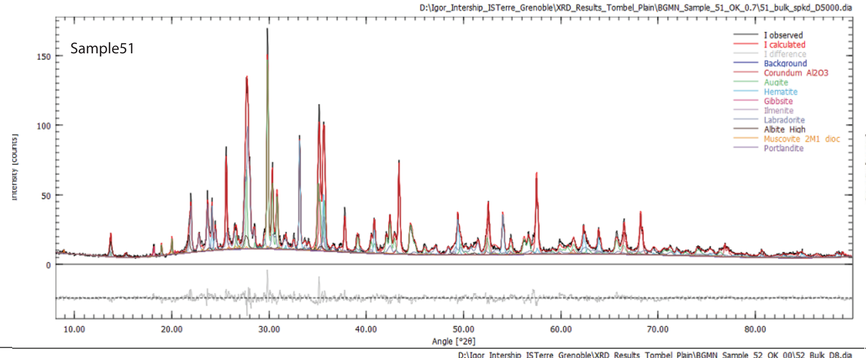

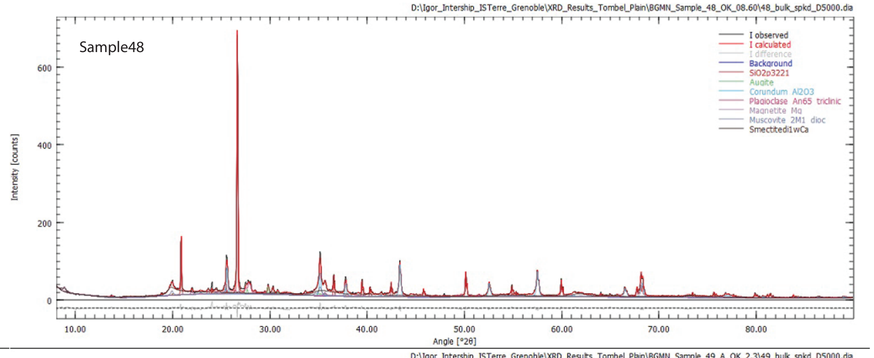

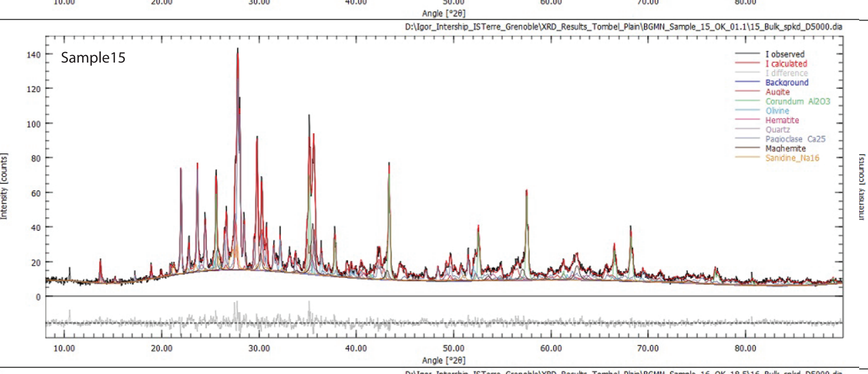

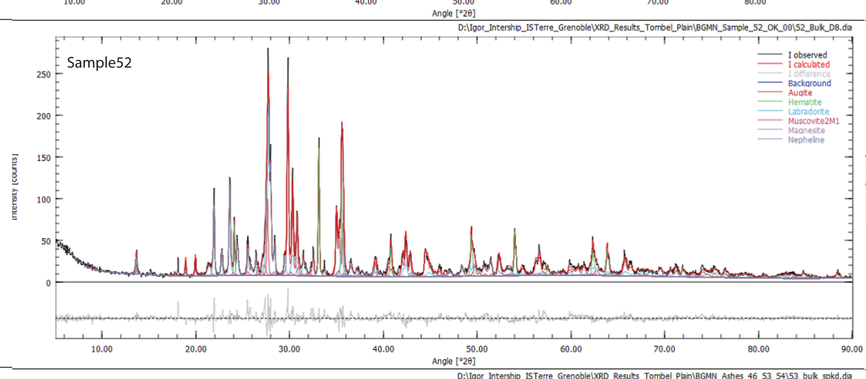

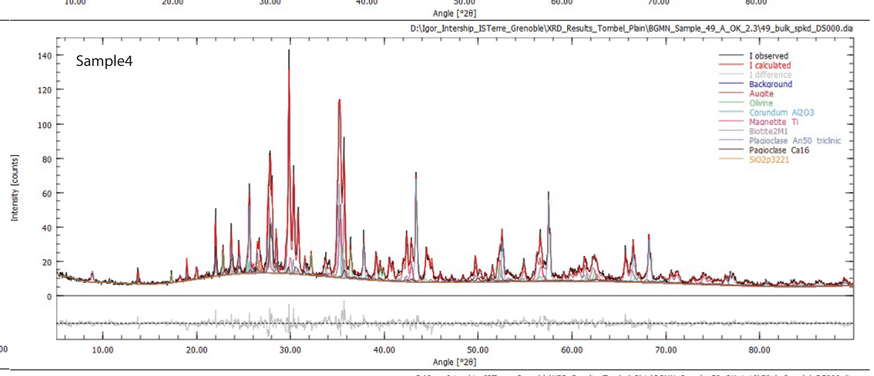

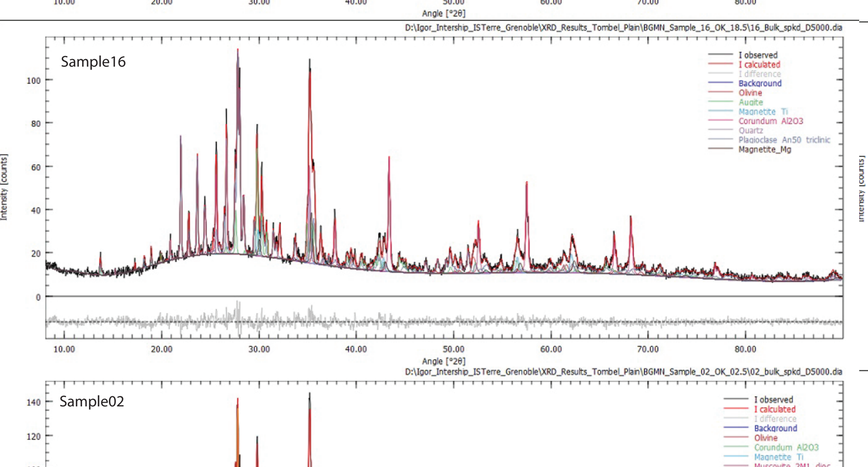

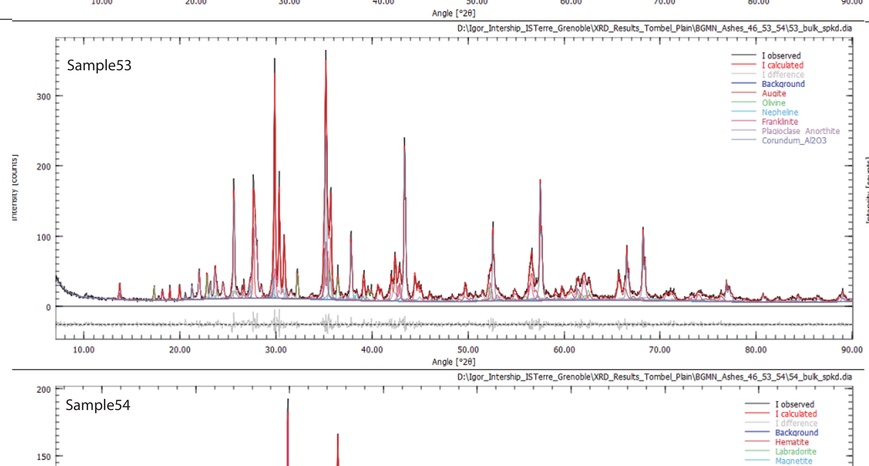

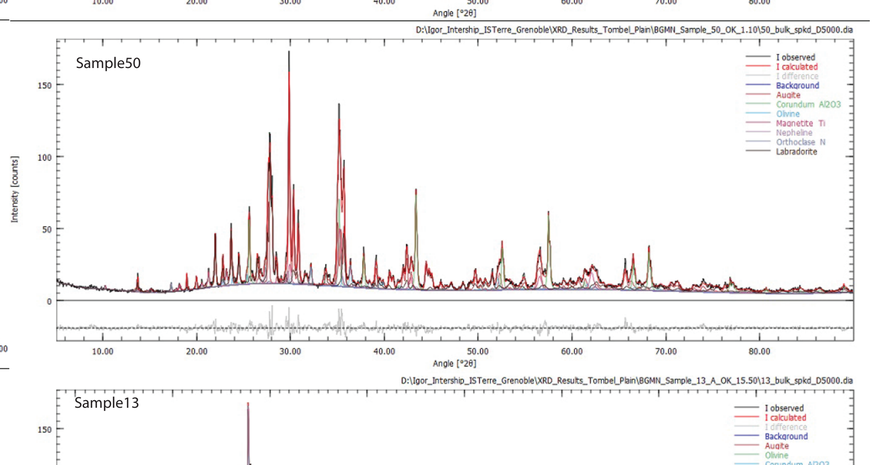

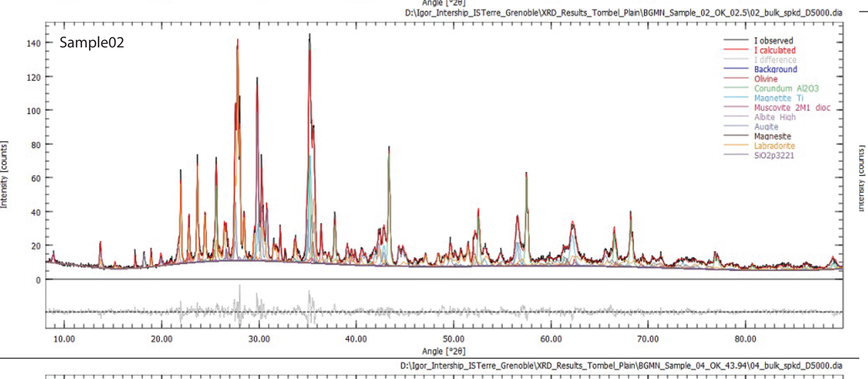

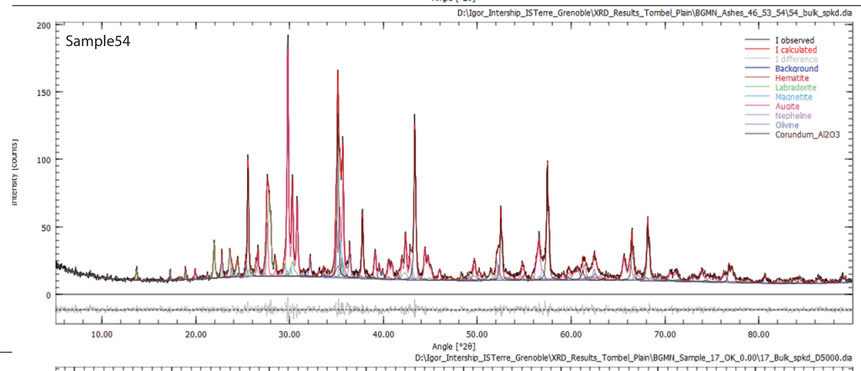

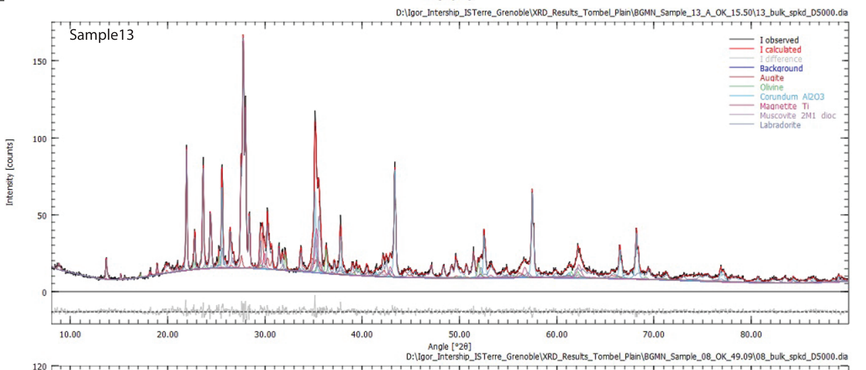

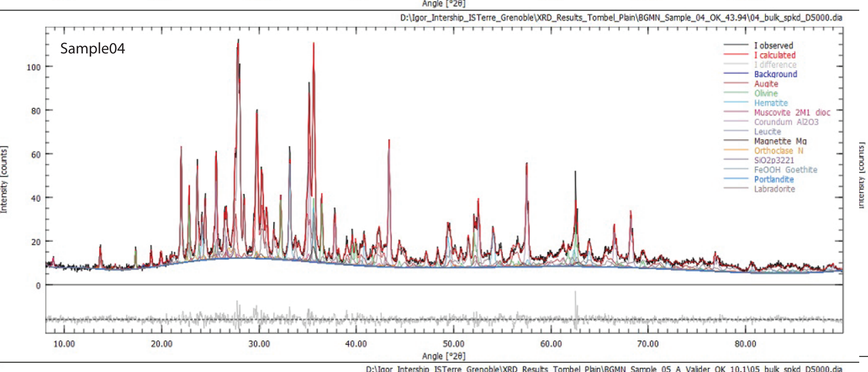

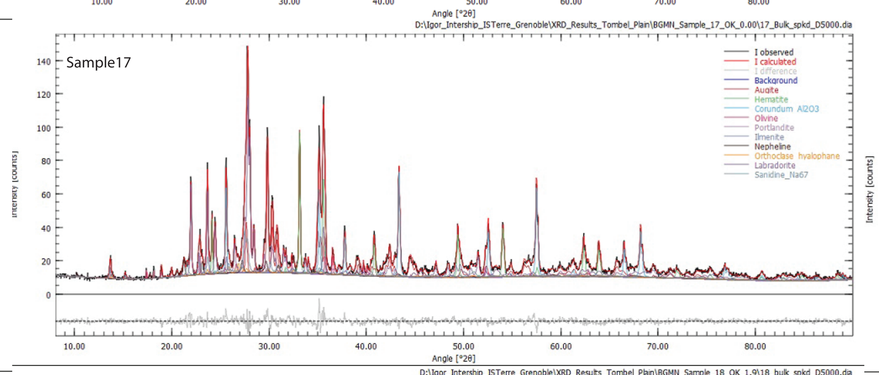

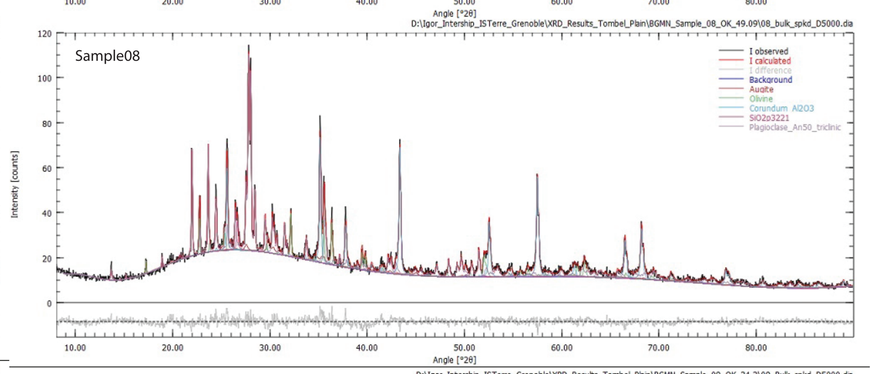

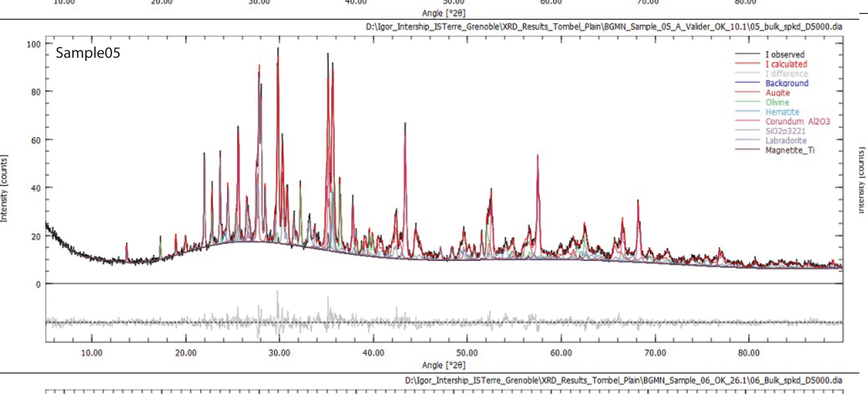

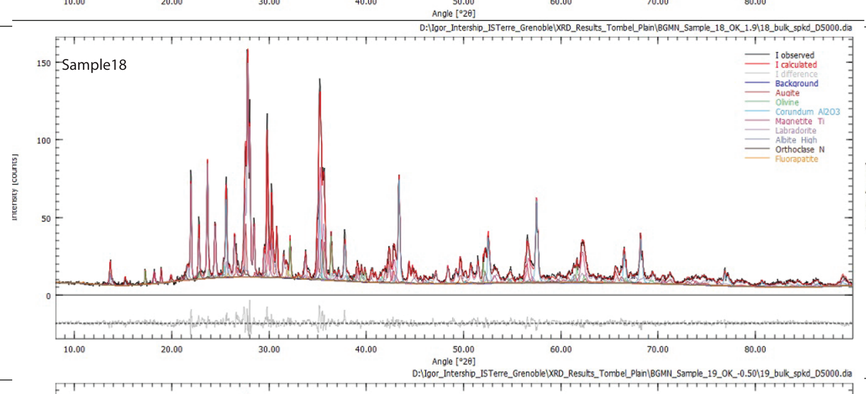

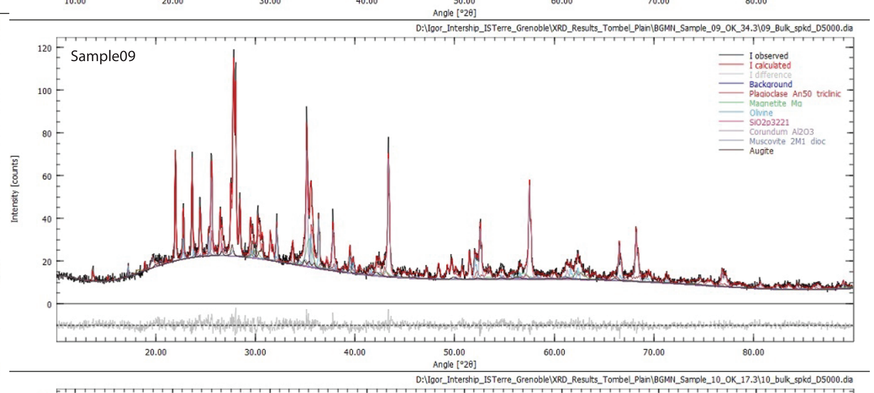

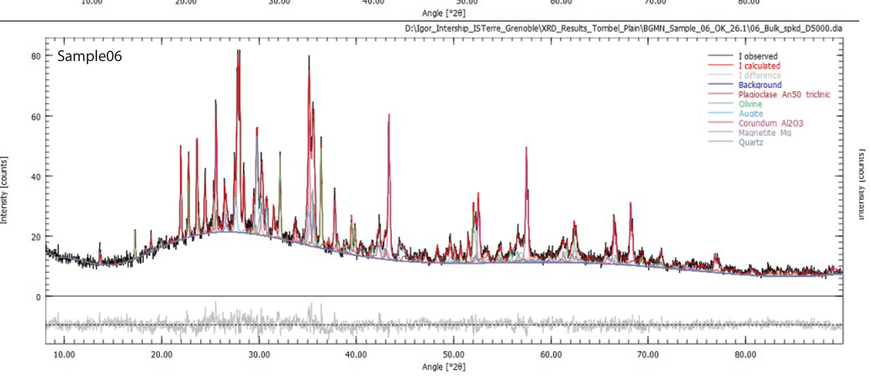

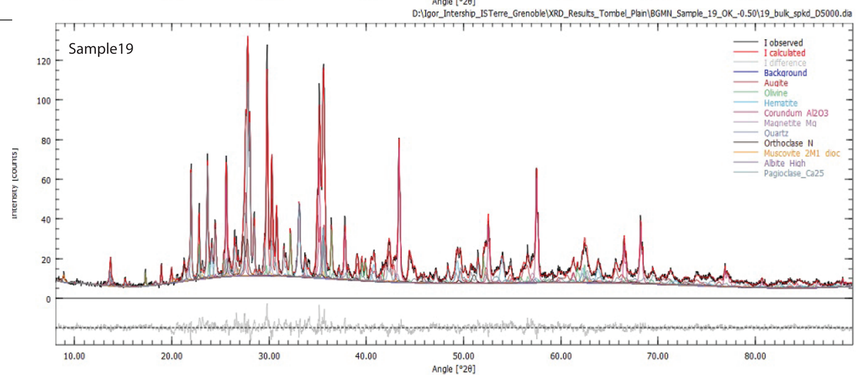

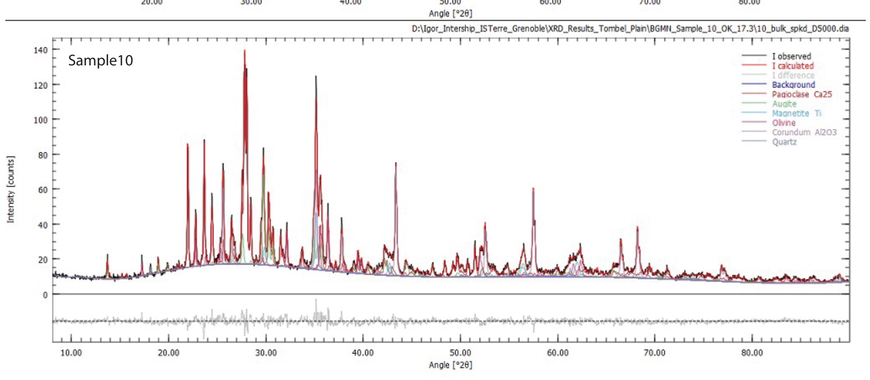

Tombel Plain

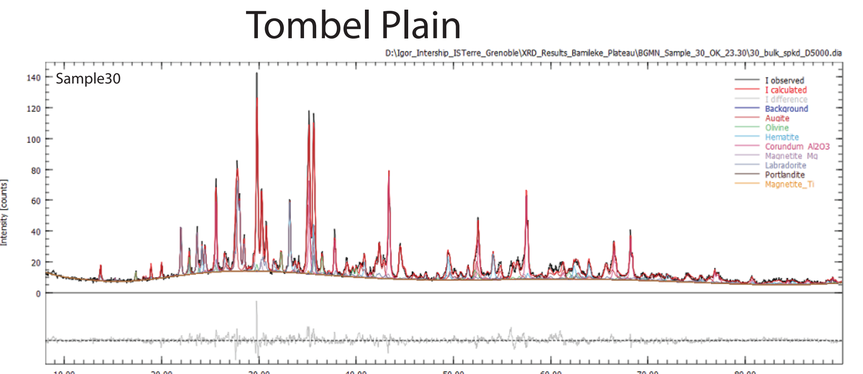

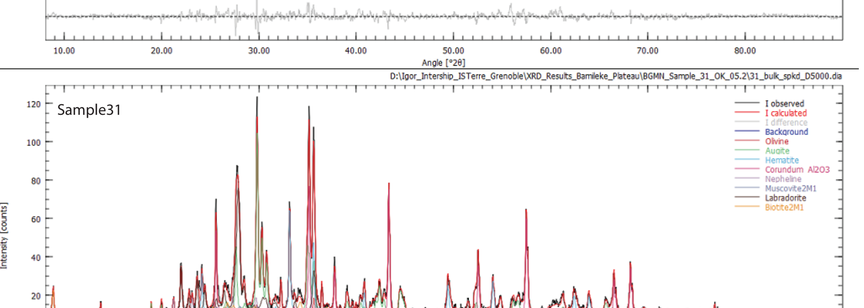

Bamileke Plateau

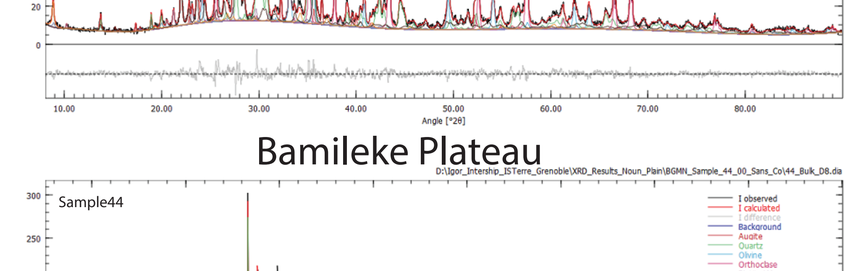

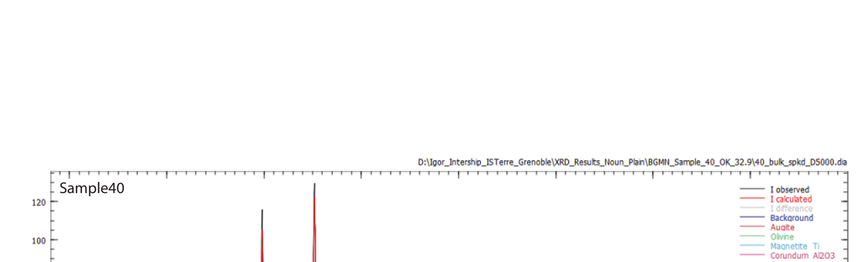

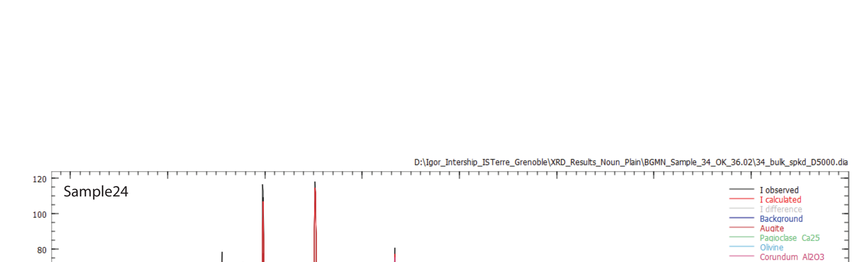

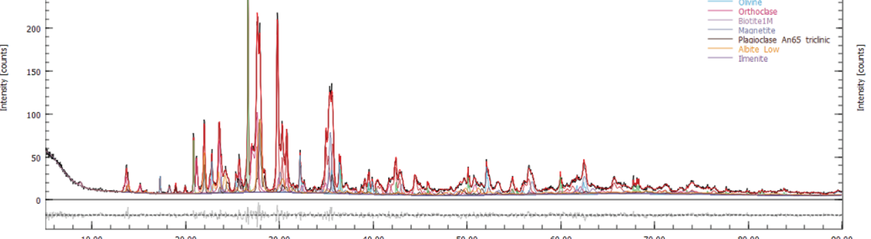

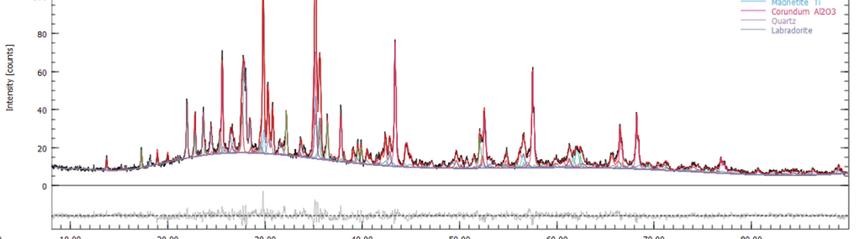

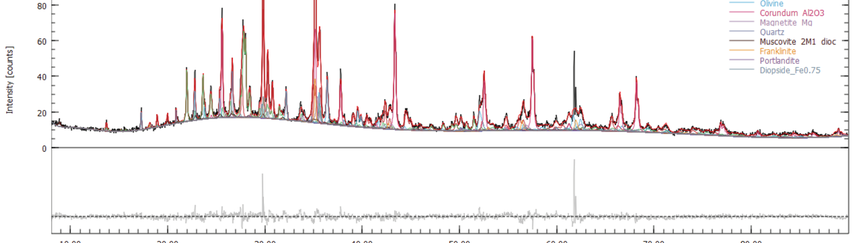

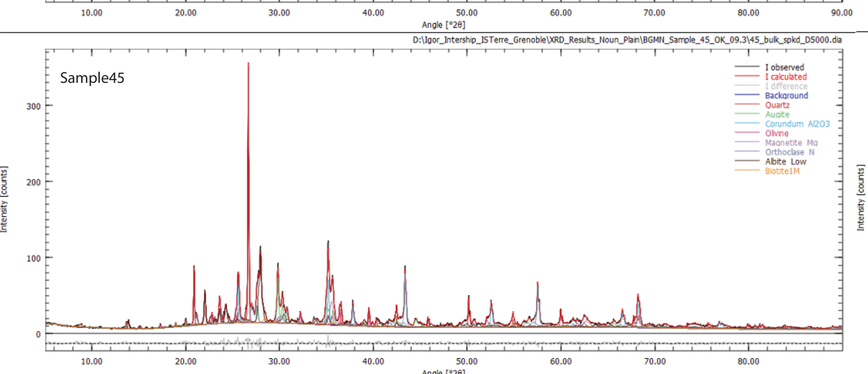

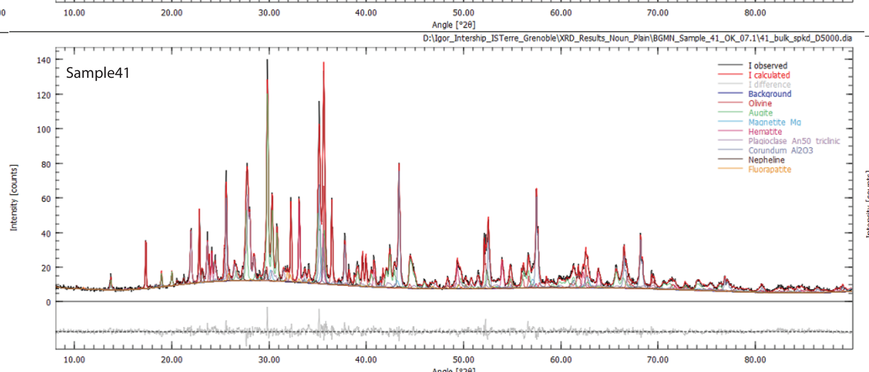

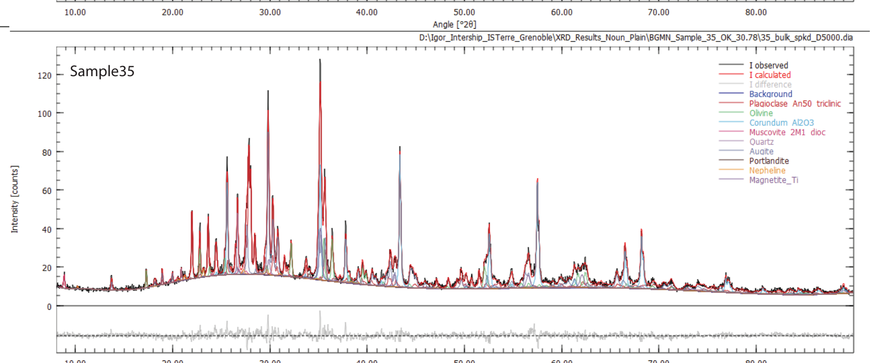

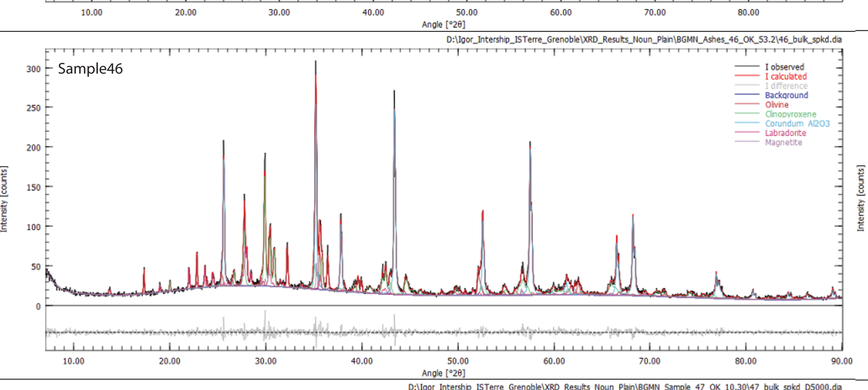

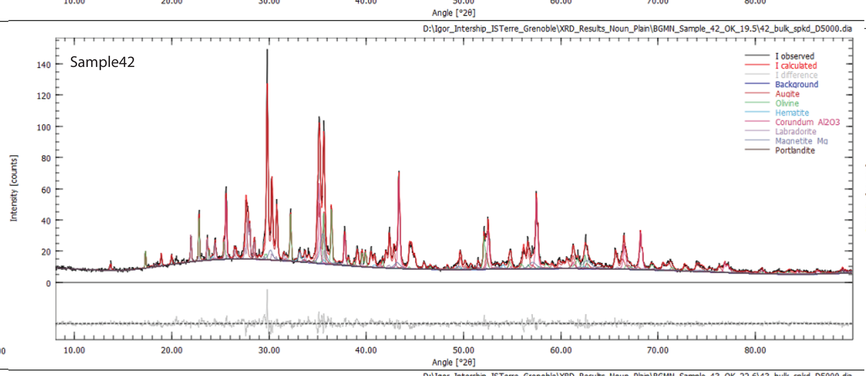

Noun Plain